SPRINGER BRIEFS IN
APPLIED SCIENCES AND TECHNOLOGY

Luciana De Simone Cividanes
Gilmar Patrocínio Thim

Functionalizing Graphene and Carbon Nanotubes

A Review

Springer

SpringerBriefs in Applied Sciences and Technology

More information about this series at http://www.springer.com/series/8884

Filipe Vargas Ferreira · Luciana De Simone Cividanes · Felipe Sales Brito
Beatriz Rossi Canuto de Menezes
Wesley Franceschi · Evelyn Alves Nunes Simonetti
Gilmar Patrocínio Thim

Functionalizing Graphene and Carbon Nanotubes

A Review

Springer

Authors
Filipe Vargas Ferreira
Instituto Tecnológico de Aeronáutica
São José dos Campos, São Paulo
Brazil

Luciana De Simone Cividanes
Instituto Tecnológico de Aeronáutica
São José dos Campos, São Paulo
Brazil

Felipe Sales Brito
Instituto Tecnológico de Aeronáutica
São José dos Campos, São Paulo
Brazil

Beatriz Rossi Canuto de Menezes
Instituto Tecnológico de Aeronáutica
São José dos Campos, São Paulo
Brazil

Wesley Franceschi
Instituto Tecnológico de Aeronáutica
São José dos Campos, São Paulo
Brazil

Evelyn Alves Nunes Simonetti
Instituto Tecnológico de Aeronáutica
São José dos Campos, São Paulo
Brazil

Gilmar Patrocínio Thim
Instituto Tecnológico de Aeronáutica
São José dos Campos, São Paulo
Brazil

ISSN 2191-530X ISSN 2191-5318 (electronic)
SpringerBriefs in Applied Sciences and Technology
ISBN 978-3-319-35109-4 ISBN 978-3-319-35110-0 (eBook)
DOI 10.1007/978-3-319-35110-0

Library of Congress Control Number: 2016945941

Printed on acid-free paper

This Springer imprint is published by Springer Nature
The registered company is Springer International Publishing AG Switzerland

Preface

Graphene and carbon nanotube (CNT) are extremely hot topics, and every day new research papers are published on this subject. This book contains complete and current reviews on graphene and CNT topics, such as synthesis, characterization, and application of functionalized materials. The characterization of functionalized materials is extremely important for the physicochemical characterization of the material obtained after the functionalization treatments. However, this characterization is rarely addressed in books or review articles. Generally, the functionalization reviews are too wide-ranging, discussing the functionalization of various materials (e.g., nanomaterials), or too specific, analyzing only one material type (e.g., only CNT) or only one functionalization agent (with some specific chemical group, e.g.). This book, however, proposes to discuss the functionalization of two of the most widely used nanomaterials in recent years: graphene and CNT. Thus, the reader will find information on graphene and CNT functionalization, using several functionalization agents, in the same book.

The Authors.

São Paulo, Brazil

Filipe Vargas Ferreira
Luciana De Simone Cividanes
Felipe Sales Brito
Beatriz Rossi Canuto de Menezes
Wesley Franceschi
Evelyn Alves Nunes Simonetti
Gilmar Patrocínio Thim

Acknowledgments

The authors gratefully acknowledge CAPES, CNPq, and FAPESP for financial support.

Contents

Chapter 1
Functionalization of Graphene and Applications

Abstract Graphene is a new member of the nanocarbon family that has revolutionized the field of materials science and has attracted much attention due to its exceptional properties. Recent progress has shown that graphene-based nanocomposites can be used in nanoelectronics, touch screens, optics, catalysis, supercapacitors, fuel cell transistors, flexible electronics, H_2 storage, and polymer nanocomposites. The functionalization is a surface modification much used to reduce the cohesive force between the graphene sheets and also to manipulate the physical and chemical properties. The aim of this book was to provide a comprehensive scientific progress of graphene, containing topics such as synthesis, characterization, and application of functionalized graphene. The characterization of the functionalized graphene is extremely important for determining the physicochemical properties of the material obtained after the functionalization treatments. However, this characterization is rarely addressed in books or in review articles. Generally, the functionalization reviews are too wide-ranging, discussing the functionalization of various materials (e.g., nanomaterials) or too specific, analyzing only one functionalization agent (with some specific chemical group, for example). This book, however, proposes to discuss the functionalization of one of the most widely used nanomaterials in recent years: graphene. Thus, the reader will find information on graphene functionalization, using several functionalization agents, in the same book.

Keywords Graphene · Synthesis · Characterization · Application · Functionalization

1.1 Graphene

1.1.1 Introduction

Over the last few years, materials have played a key role in various industrial sectors of technology, such as aerospace, aeronautical, automotive, medical, and

F.V. Ferreira et al., *Functionalizing Graphene and Carbon Nanotubes*,
SpringerBriefs in Applied Sciences and Technology,
DOI 10.1007/978-3-319-35110-0_1

sensors. Therefore, understanding the relationship between structures and material properties has become increasingly important to develop novel materials with improved properties in order to meet these needs (Mittal et al. 2015). In this context, nanotechnology and nanoscience have shown great development, and as a result, many knowledge fields based on the macromaterials are currently exploited and manipulated at nanoscale (Ferreira et al. 2015). As a result, several nanomaterials with different sizes and shapes have appeared during the past few decades (Wang et al. 2015a).

A new member of the nanocarbon family has revolutionized the field of materials science: graphene. Graphene is the mother element of some carbon allotropes (Fig. 1.1), including graphite, carbon nanotubes, and fullerenes (Geim and Novoselov 2007; Chia et al. 2015; Li et al. 2015; Kim et al. 2010; Kuila et al. 2012). Graphene was theoretically established in 1940 (Wallace 1947), while Boehm and coworkers, in 1962, separated thin carbon layers from graphite oxide (Boehm et al. 1962; Rohini et al. 2015). In 2010, the Nobel Prize in Physics was awarded to Andre Geim and Konstantin Novoselov for the successful preparation and isolation of graphene samples of highly oriented pyrolytic graphite (Novoselov et al. 2004; Rohini et al. 2015; Sanchez et al. 2012; Mao et al. 2013). Graphene is an atomically thick 2D planar sheet of carbon atoms arranged in a sp^2-hybridized configuration and densely packed in a honeycomb structure (Liu et al. 2015b; Suggs et al. 2011; Allen et al. 2010). These sp^2-hybridized carbon bonds contain in-plane σ bonds and out-of-plane π bonds (Mao et al. 2013).

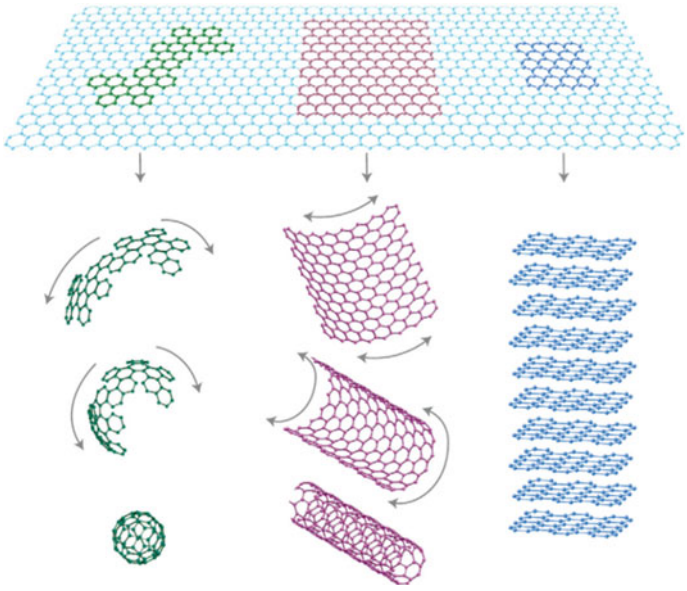

Fig. 1.1 Graphene is the basis of all graphitic forms, and it is a 2D building material for carbon materials of all other dimensionalities. It can be wrapped up into 0D buckyballs, rolled into 1D nanotubes, or stacked into 3D graphite (Geim and Novoselov 2007)

Graphene is relatively new and the "thinnest" known material. The enormous amount of interest worldwide is due to its extraordinary properties: thermal conductivity (as high as 3000 Wm^{-1} K^{-1}) (Compton et al. 2011), electrical conductivity of 2×10^3 S cm^{-1} (Rohini et al. 2015), excellent optical transparency (~97.7 %) (Liao et al. 2014), mechanical stiffness (>1000 GPa) (Rohini et al. 2015), Young's modulus of 1 TPa (Wang et al. 2012b), high charge mobility (>200,000 cm^2 V^{-1} s^{-1}) (Liu et al. 2009), high surface area (2630 m^2 g^{-1}) (Liu et al. 2015b), and high thermal stability up to approximately 600 °C (Rohini et al. 2015), as well as (Liao et al. 2014). These properties make them viable candidates for a wide variety of potential applications, such as transparent conductive electrodes (Wang et al. 2015a), energy storage devices (Lv et al. 2015), drug delivery (Pinto et al. 2013), composite material (Rohini et al. 2015), and tissue engineering (Goenka et al. 2014), as well as (Liu et al. 2015b; Rohini et al. 2015; Kuila et al. 2012).

Graphene in general is expensive when compared to other carbon-based nanofillers, such as carbon nanotubes. However, some graphene derivatives, such as graphene oxide (GO), are inexpensive (Rohini et al. 2015). GO is a graphene analog with many functional groups that make the physical and chemical properties of GO largely different from those of graphene (Toda et al. 2015).

1.1.2 Synthesis

The large-scale production of graphene with high-quality sheets and defect free has become an urgent challenge as well as a labor-intensive task (Kuila et al. 2012; Mittal et al. 2015). In this context, to meet the demanding requirements, extensive research efforts have focused on developing large-scale methods of graphene synthesis (Green and Hersam 2009; Jayasena and Melkote 2015). Numerous graphene synthesis routes have been reported in the literature, but only six will be discussed here: mechanical exfoliation, chemical vapor deposition (CVD), reduction of graphite oxide, epitaxial growth on SiC, electrochemical exfoliation, and carbon nanotube unzipping. Figure 1.2 illustrates some types of graphene synthesis routes, outlining the general real-life applications (Mittal et al. 2015).

The advantages and disadvantages of each method are summarized in Table 1.1.

1.1.2.1 Mechanical Exfoliation

Mechanical exfoliation is the first method used for graphene preparation (Novoselov et al. 2004; Mittal et al. 2015; Rohini et al. 2015). This method is a simple peeling process where mechanical energy is primarily used to exfoliate graphite and to separate the stable graphene sheets (Fig. 1.3) (Yang et al. 2013; Singh et al. 2011). However, the yield obtained through mechanical exfoliation is not suitable for large-scale production of graphene (Jayasena and Melkote 2015).

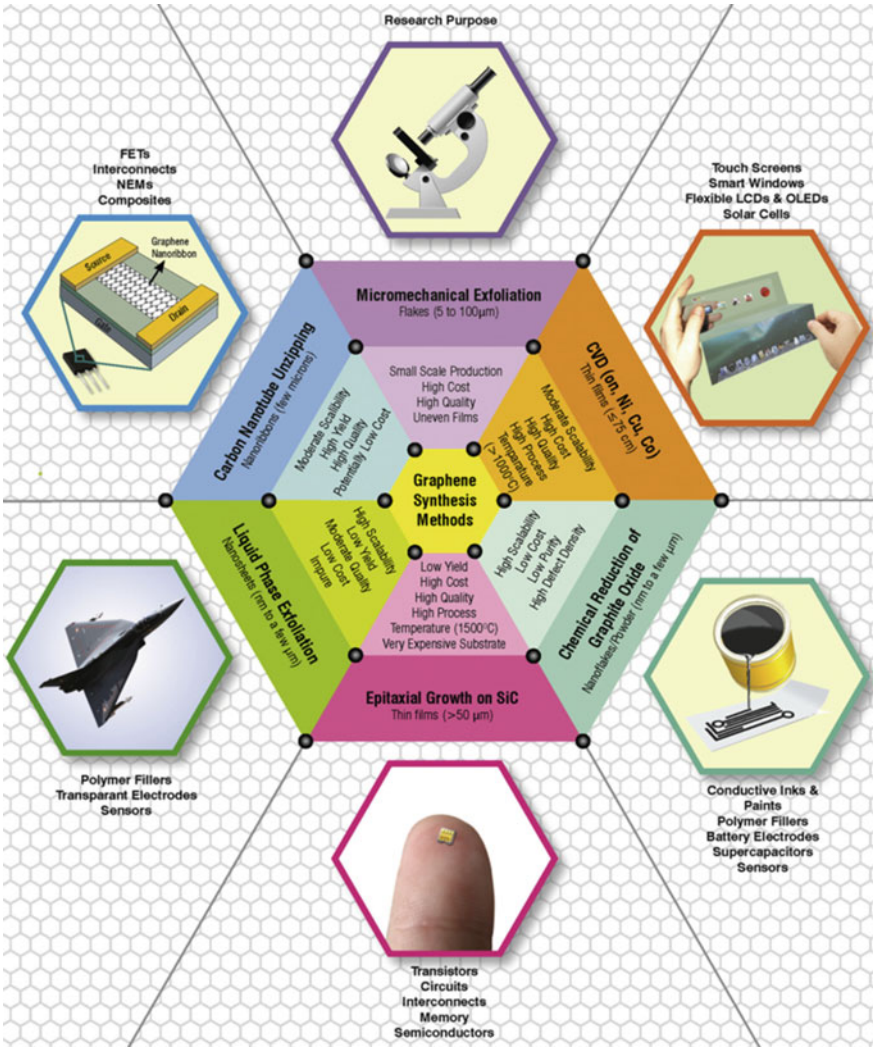

Fig. 1.2 Scheme depicting various conventional synthesis methods of graphene along with their important features, and their current and potential applications (Mittal et al. 2015)

Therefore, an alternative to this is to produce large quantities of graphene via chemical vapor deposition.

1.1.2.2 Chemical Vapor Deposition (CVD)

The production of graphene by chemical vapor deposition was first reported in 2006 by Somani's group (Somani et al. 2006) and is today one of the most promising

Table 1.1 Advantages and disadvantages of several methods used in the synthesis of graphene

Method	Advantage	Disadvantage	References
Mechanical exfoliation	High quality, low cost, poor control	Tens of microns in size, small-scale production	Chatterjee et al. (2015), Kim et al. (2010), Jayasena and Melkote (2015)
Chemical vapor deposition (CVD)	High quality, large-scale production, good control	High cost, hazardous chemicals	Chatterjee et al. (2015), Frank and Kalbac (2014), Kim et al. (2010), Singh et al. (2011)
GO reduction	Cheap, large-scale production, moderate control	Hazardous chemicals, poor quality	Chatterjee et al. (2015), Kim et al. (2010), Singh et al. (2011)
Epitaxial growth on SiC	High quality, good control, large area of graphene	Very small-scale, high-temperature process	Chatterjee et al. (2015); Kim et al. (2010), Kumar et al. (2016), Zhang et al. (2015a)
Electrochemical exfoliation	Good control	Poor quality	Kim et al. (2010), Yu et al. (2015), Parvez et al. (2015)
Carbon nanotube unzipping	Good control	High cost, very small-scale production	Chatterjee et al. (2015), Kim et al. (2010), Hirsch (2009)

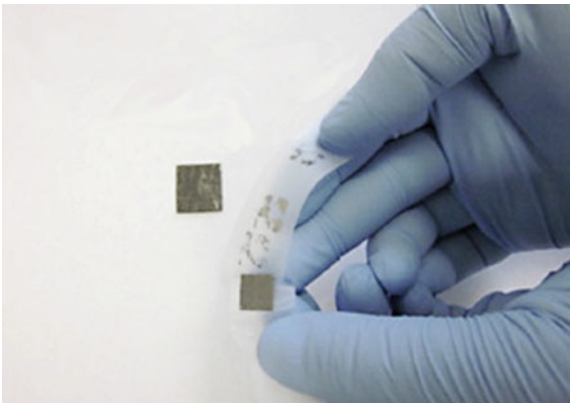

Fig. 1.3 Scotch tape method of graphene synthesis from highly oriented pyrolytic graphite (HOPG) block (Mittal et al. 2015)

techniques for large-scale production of graphene (Singh et al. 2011). Somani's group synthesized few-layer graphene films using camphor as precursor and Ni foils as catalyst (Mittal et al. 2015; Singh et al. 2011). Later on, several new advances in this synthesis procedure were reported using different metal substrates, e.g., Cu (Liu et al. 2015e), Pt (Karamat et al. 2015), Mo (Grachova et al. 2014), Ir (Coraux et al. 2008), or Au (Oznuluer et al. 2011). Several metals can be used as catalyst in CVD graphene growth, but Cu and Ni are most widely used for scale-up graphene production (Frank and Kalbac 2014; Mittal et al. 2015).

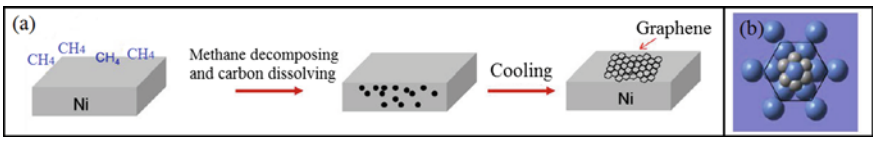

Fig. 1.4 **a** Schematic diagram of graphene formation on Ni. **b** Schematic diagram of graphene atoms (smaller atoms) on Ni (111) lattice (larger atoms). (Adapted from Zhang et al. 2013)

In general, CVD of graphene is performed in a gas phase where a precursor (usually a small hydrocarbon) reacts with a catalyst in a reaction chamber at a high temperature (range from several hundred degrees Celsius up to the melting point of the catalyst metal). Thus, the graphene is formed on the catalyst surface (Frank and Kalbac 2014). When nickel is used as a catalyst, a Ni substrate is placed in a CVD chamber at a vacuum and temperature below 1000 °C in an atmosphere of diluted hydrocarbon gas. The deposition process starts when carbon deposits on a Ni surface after the cooling process (Mittal et al. 2015). The thickness and crystalline ordering of the precipitated carbon (graphene layers) are controlled by the cooling rate and the concentration of carbon dissolved in the nickel (Singh et al. 2011). Figure 1.4 shows the graphene formation by chemical vapor deposition using Ni as substrate.

1.1.2.3 Reduction of Graphite Oxide

Another promising alternative to produce large quantities of graphene is the reduction of the graphene oxide (GO) produced by Hummers' method, which is illustrated in Fig. 1.5 (Hummers and Offeman 1958). The reduction process can be performed thermally (Ho and Wang 2015; Compton et al. 2011) or chemically (Yuan et al. 2016; Mittal et al. 2015; Rohini et al. 2015). GO is synthesized by Hummers' method through a graphite oxidation using strong oxidizing agents (Singh et al. 2011). The thermal reduction of graphene from GO can be achieved using a microwave. In this method, GO is dispersed in water and then sonicated with *N*,*N*-dimethylacetamide (DMAc). Next, GO suspensions are subjected to

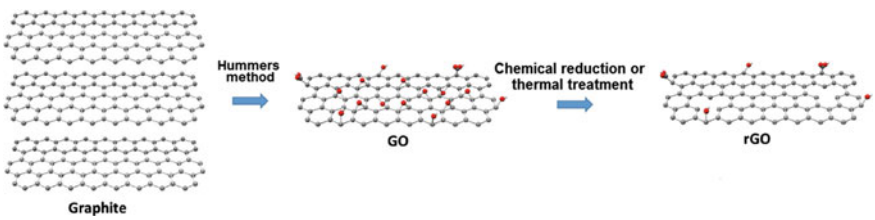

Fig. 1.5 Oxidation of graphite to graphene oxide (GO) and reduction to reduced graphene oxide (rGO). (Adapted from Toda et al. 2015)

different microwave exposure time intervals (Rohini et al. 2015). Chemical reduction of GO sheets may be obtained using several reducing agents (Stankovich et al. 2007; Shin et al. 2009). However, hydrazine hydrate is one of the most commonly used reagents to produce very thin graphene sheets (Singh et al. 2011; Rohini et al. 2015).

1.1.2.4 Epitaxial Growth on SiC

The epitaxial growth of graphene is based on the sublimation of Si from a surface of a single-crystalline SiC, leaving a face rich in carbon that forms graphene (Zhang et al. 2015a). This method is very promising due to the production of large size graphene sheets, elevated purity, and uniform properties (Kumar et al. 2016). Furthermore, graphene produced by epitaxial growth is almost defect free (Liu et al. 2015e).

Several works in recent years have demonstrated the possibility of growing perfectly controlled layers of graphene on SiC using several procedures, such as under ultra-high vacuum (UHV) conditions, under Ar and N_2 atmosphere (Kumar et al. 2016; Çelebi et al. 2012; Zarotti et al. 2016; Zhang et al. 2013). However, high temperatures (about 1500 °C) hamper the large-scale production of graphene (Mittal et al. 2015; Kim et al. 2010) due to the quick diffusion of silicon from the SiC surface at high temperatures, under non-equilibrium conditions (Zarotti et al. 2016).

1.1.2.5 Electrochemical Exfoliation

The electrochemical exfoliation is a green method of graphene production and was first reported in 1976 (Besenhard 1976; Parvez et al. 2015; Bose et al. 2014). In this method, graphite is oxidized in a mixture of sulfuric and nitric acid (Mittal et al. 2015) and then exfoliated in an electrochemical device (Mittal et al. 2015; Yu et al. 2015). Figure 1.6 shows the electrochemical experimental setup.

The electrochemical method offers some advantages over the other methods, such as the simple one-step operation and control of the synthesis, functionalization, and exfoliation process (Parvez et al. 2015). However, the graphene produced by the electrochemical method presents a number of defects, which modify the electronic properties of graphene (Mittal et al. 2015; Kim et al. 2010).

1.1.2.6 Carbon Nanotube Unzipping

Carbon nanotubes are considered graphene sheets rolled up in seamless tubes (Jiao et al. 2009). Therefore, it would seem natural that CNTs can be unzipped to obtain graphene (Terrones et al. 2010). The first method to obtain graphitic nanoribbons from CNT unzipping was published by Márquez and coworkers (Márquez et al.

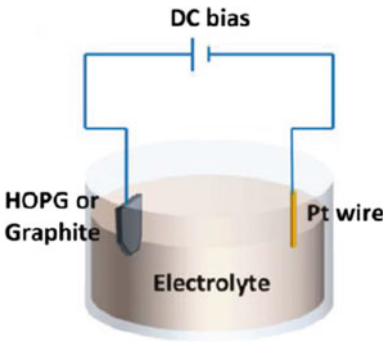

Fig. 1.6 Schematic illustration of a typical setup for the electrochemical exfoliation of graphite. (Adapted from Yu et al. 2015)

2009). In this method, carbon nanotubes were opened longitudinally by intercalation of lithium and ammonia followed by exfoliation. Two other new methods appeared two weeks later: solution-based oxidative (Kosynkin et al. 2009) and Ar plasma etching (Jiao et al. 2009). Since then, various other methods have been successfully applied to produce graphene from the CNT opening (Elías et al. 2010; Terrones et al. 2010). Figure 1.7 shows different methods to unzip carbon nanotubes (Terrones et al. 2010).

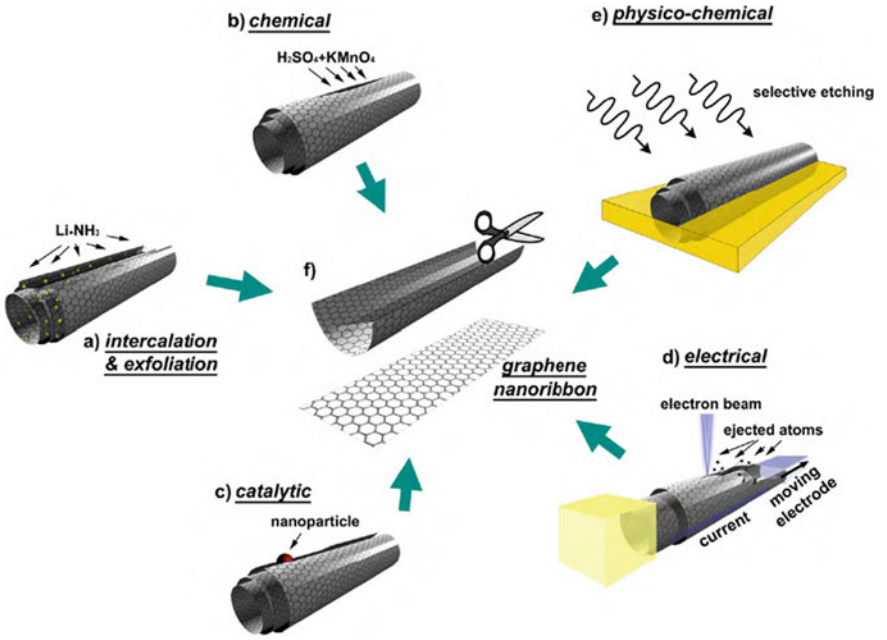

Fig. 1.7 Schematics and representative images of several methods for unzipping CNTs into graphene nanoribbons (Terrones et al. 2010)

Carbon nanotube unzipping methods are very appealing, since they are simple and lead to well-defined shaped graphene (Kim et al. 2010; Hirsch 2009). However, these methods are not suitable for mass production of graphene (Chatterjee et al. 2015). Moreover, starting materials are expensive (Kim et al. 2010).

1.1.3 Graphene Functionalization

As summarized above, the properties and applications of graphene can be controlled by synthetic conditions. Each preparation method not only has advantages and drawbacks over the other methods, but also provides flexible graphene for various applications (Mittal et al. 2015; Liu et al. 2015e). Furthermore, the properties and applications of graphene can also be adjusted by other parameters, such as number of layers, dimensions, and in particular surface modification (Liu et al. 2015b).

Surface modification is one of the main methods used to reduce the cohesive force between the graphene sheets and also to manipulate the physical and chemical properties of graphene (Layek and Nandi 2013; Boukhvalov and Katsnelson 2009). It provides numerous additional functions to graphene sheets, hence playing a crucial role in their potential commercial applications in band gap engineering, gas sensing, spintronics, and so on (Chia et al. 2015; Sayin et al. 2015; Liu et al. 2015d; Chatterjee et al. 2015; Singh et al. 2011; Han et al. 2007).

Generally speaking, surface functionalization could be summarized as two main approaches: covalent functionalization, which is related to covalent bond formations, and non-covalent functionalization, which is associated with van der Waals forces (Boukhvalov and Katsnelson 2009). The works in the literature are often related to covalent functionalization because it forms a stronger modification of geometric and electronic properties of graphene (Boukhvalov and Katsnelson 2009).

1.1.3.1 Covalent Functionalization

Covalent modification offers great potential to develop new functional materials, structures, and devices for interesting and promising applications (Kim and Grossman 2015). The covalent linkage between unsaturated π bonds of carbon and other functional groups is the base of a covalent functionalization (Mittal et al. 2015). The functionalization occurs by the reaction of π orbitals transforming sp^2 bonds into sp^3 (Liu et al. 2015b; Haldar et al. 2012; Niyogi et al. 2010). Therefore, graphene is able to covalently bond with other species since it is chemically unsaturated (Mao et al. 2013). However, this functionalization may be accompanied by a deterioration of the electron transport due to the conversion of sp^2 into sp^3 carbon (Layek and Nandi 2013; Sayin et al. 2015). Figure 1.8 shows a schematic illustration of graphene covalent functionalization.

Within the last few years, graphene covalent functionalization has been intensively investigated theoretically (Suggs et al. 2011). For instance, Li et al. (2011)

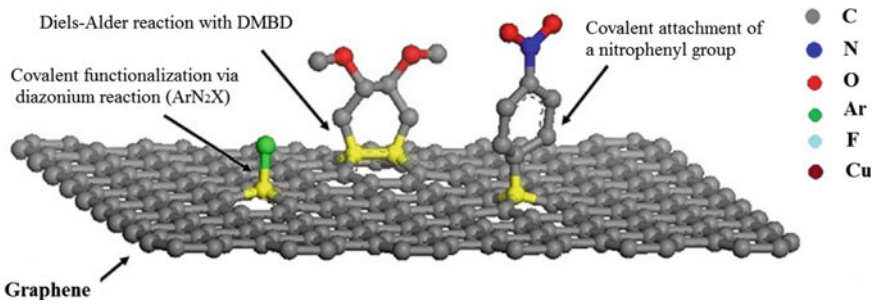

Fig. 1.8 Schematic illustration of covalent functionalization of graphene. (Adapted from Mao et al. 2013)

studied the graphene functionalization by first-principle calculations. The authors considered functionalization only on one side with F (F-graphene), O (O-graphene), and OH (OH-graphene) and on both sides with F and H (F-graphene-H), O, and H (O-graphene-H). The results demonstrated that the functionalized graphenes allow much larger spin current density with lower fabrication requirements, when compared with ultra-narrow graphene nanoribbon spintronics devices. Using classical and quantum mechanical calculations, Kim and Grossman (2015) showed that chemical functionalization of graphene can improve the electronic properties (thermoelectric power factor, $PF = S^2\sigma$) compared to pristine graphene.

Using molecular and lattice dynamics simulations in another work, Kim et al. (2012) investigated the effects of graphene functional groups on thermal transport. Graphene was functionalized with H atoms and hydrocarbon chains (pentane C_5H_{12}) on both sides in an alternating manner. The simulation results demonstrated that the chemical functionalization plays a significant role in the thermal transport of 2D materials. The 2D periodic patterns of a graphene sheet suppress the thermal conductivity as all atoms can be functionalized in the 2D system. In contrast to a 3D structure where only surface atoms can be functionalized, consequently, a minor influence on thermal transport is observed.

Covalent functionalization of graphene has also been investigated experimentally. In the experimental study, graphene oxide (GO) is synthesized by the Hummers' method and subsequently functionalized. The Hummers' method introduces some oxygenated species (carboxyl, epoxy, and hydroxyl groups) during the graphite oxidation processes (Mao et al. 2013). Therefore, the presence of these functional groups facilitates the covalent molecular functionalization of graphene (Hossain et al. 2012).

Maktedar et al. (2014) studied the antibacterial activity of modified graphene oxide. Sonochemical waves were employed to exfoliate GO. After that, GO was functionalized with 6-aminoindazole forming f-(6-AIND) GO. The results showed that f-(6-AIND) GO is an antibacterial and antifungal agent.

Lin et al. (2011) studied the capacitance of the functionalized graphene prepared by controlled reduction of graphene oxide. GO was synthesized using the Hummers' method, and GO was functionalized using dimethylformamide (DMF) in a solvothermal method. The functionalized graphene showed the specific capacitance up to 276 F/g, which is much higher than the benchmark materials.

Mohanty and Berry (2008) reported the fabrication of chemically modified graphenes (CMGs) in a single-bacterium biodevice. CMGs were synthesized using GO and plasma-modified graphene-amine (PGA) on a silica substrate. GOs were synthesized from graphite flakes by the modified Hummers' method. PGA was synthesized either by exposing the graphite flakes to ammonia (or nitrogen plasma) followed by exfoliation. Initially, the substrate was exposed to oxygen plasma and then functionalized with a monolayer of (3-aminopropyl) triethoxysilane to make the silica surface positively charged with tethered amine groups. Choi et al. (2010) created sulfonate ($-SO_3$) groups in the graphene surface using microwave-assisted sulfonation.

Xue et al. (2015) investigated the catalytic performance of GO functionalized with ethylenediamine (N-GO) in the Knoevenagel condensation reactions. According to the results, pure GO showed almost no catalytic activity for the Knoevenagel condensation reactions of benzaldehyde. On the other hand, after functionalization, the conversion of benzaldehyde into N-GO samples significantly increased.

Although the electronic and chemical properties of graphene can be effectively tailored by covalent functionalizations, the properties related to the transport of electrons or phonons may be disrupted (Layek and Nandi 2013; Mao et al. 2013). An alternative to overcome this drawback is to use non-covalent functionalizations since they cause less perturbation to the graphene π-conjugated structure (Mao et al. 2013).

1.1.3.2 Non-covalent Functionalization

In summary, surface modification of graphene is a versatile method to manipulate its physical and chemical properties, essential condition to expand their potential commercial applications (Layek and Nandi 2013). The native electronic structure and physical properties of graphene can be effectively modified by covalent functionalization. However, this functionalization may be accompanied by some damage on the graphene electron conjugation (Sayin et al. 2015; Kuila et al. 2012). Non-covalent functionalizations of graphene are nondestructive methods, since the electronic, chemical, physical, and mechanical properties of the pristine graphene are preserved after the modification (Mao et al. 2013). However, the efficiency of load transfer and force between the wrapping molecules is weaker than the covalent functionalization (Layek and Nandi 2013). Therefore, the type of functionalization of graphene should be carefully selected based on the specific performances.

Non-covalent functionalizations with different organic compounds have become very attractive to make graphene soluble in different solvents, obtaining high

dispersion. Non-covalent functionalizations are based on π interaction, attaching functional groups without disturbing the electronic network. Many π interactions can be developed as follows:

(1) Nonpolar gas-π interaction: In this, the functionalizing molecule is a gas. The gas–graphene chemical bonding is based on both electrostatic and dispersion energies.
(2) π–π interaction: Because graphene and the functionalizing agent have similar electron densities, the interaction is predominated by dispersion or induction.
(3) Cation-π interaction: Because functionalizing agent is a metallic cation, the interaction is based on the induction energies.
(4) Anion-π interaction: The contribution of the dispersion energies is substantial in the anion-π complexes.

The different types of non-covalent functionalization should be carefully selected based on the specific performances (Jo et al. 2015; Georgakilas et al. 2012).

1.1.3.3 Other Methods of Graphene Functionalization

Besides the covalent and non-covalent functionalizations, other methods of graphene functionalization have received considerable attention due to their wide range of applications (Liu et al. 2015b). For example, Chen et al. (2015) studied the electrochemical performance of functionalizing graphene oxide with Co_2SnO_4 (Co_2SnO_4/G). GO was synthesized from natural graphite by a modified Hummers' method. Co_2SnO_4/G nanocomposites were synthesized using the hydrothermal method. The nanocomposites exhibited an improved electrochemical performance, such as high reversible capacities, good cycling stability, and excellent performance rate compared to pure Co_2SnO_4 nanoparticles. Cai et al. (2015) prepared the nanocomposite of SnO_2 dodecahedral nanocrystals (DNCs) anchored on graphene sheets (GS) as an advanced anode for high-performance lithium-ion batteries. Graphene oxide was prepared from graphite powder via modified Hummers' method. The composite of SnO_2 DNCs anchored on GS was synthesized by a facile hydrothermal method. The SnO_2 DNCs-GS nanocomposite exhibited a significant Li battery performance compared with pure SnO_2 DNCs. Wang et al. (2015b) functionalized two-dimensional reduced graphene oxide (2D rGO) with MnO_2 (MnO_2/rGO) by the hydrothermal method and studied their activity in a catalytic ozonation. The results showed that the catalytic efficiency of MnO_2/rGO was superior to either MnO_2 or rGO in the catalytic ozonation of 4-nitrophenol. This method was employed by other authors for graphene functionalization with Co_3O_4 (Dong et al. 2012) and $Co(OH)_2$ (Wang et al. 2012a).

Furthermore, other methods are used to prepare the functionalized graphene: Hassan et al. (2015) reported the microwave-assisted synthesis of metal nanoparticles (Pd, Cu, and PdCu) dispersed on the graphene sheets. The method allows the simultaneous reduction of GO and various metal salts. Using this method, many

types of metallic and bimetallic nanoparticles can be dispersed on graphene sheets to create novel nanocatalysts supported on the large surface area of the thermally stable 2D graphene (Liu et al. 2015b). Song et al. (2012) prepared Fe_3O_4—GO nanocomposites by a chemical coprecipitation method. The results show that the nanocomposites exhibited a good activity for the electrooxidation of cysteine and N-acetyl cysteine in 0.1 M NaOH.

In addition, functionalization with Fe_3O_4 was also reported in other works (Wu et al. 2012). Renteria and coworkers used Fe_3O_4 nanoparticles for the functionalization of graphene (2015). Graphene nanocomposites were synthesized by a scalable technique based on liquid-phase exfoliation. The authors showed that Fe_3O_4 nanoparticles aligned the graphene fillers under an external magnetic field. The graphene filler alignment resulted in a strong increase in the thermal conductivity of the composites.

1.1.4 Graphene Applications

Graphene has attracted much attention due to its exceptional properties, especially in electronics, making this material an attractive candidate for future nanoelectronics (Xia et al. 2010; Georgakilas et al. 2012). Currently, graphene-based nanocomposites are studied to be used in nanoelectronics, touch screens, optics, catalysis, supercapacitors, fuel cell transistors, flexible electronics, H_2 storage, and polymer nanocomposites (Sayin et al. 2015; Kuila et al. 2012).

In the following paragraphs, some graphene applications will be discussed in more detail.

1.1.4.1 Graphene/Polymer Matrix Composites

Graphene plays an important role in the development of nanocomposites due to its high specific surface area, unique graphitized plane structure, and excellent mechanical, electrical, magnetic, and thermal properties. Graphene and polymer composites have a wide range of exciting applications. However, as mentioned earlier, chemical functionalizations are essential to achieve a high performance of the nanocomposite, due to a uniform dispersion and enhanced compatibility with the matrix (Liu et al. 2015c).

1.1.4.2 Mechanical Applications

The main objective of a high-performance polymer composite for mechanic application is the balance between strength and toughness, and graphene improves these two mechanical properties when it is added into a polymer. These properties

together with the large specific surface area make graphene excellent reinforcing nanofillers (Zhang et al. 2015b).

Yadav and Cho (2013) studied the properties of nanocomposites of graphene nanoplatelets and polyurethane (PU) by the incorporation of the functionalized graphene nanoplatelets into a polyurethane (PU) followed by an "in situ" polymerization. Graphene was functionalized by a coupling reaction with 4-aminophenethyl alcohol. Their results showed a formation of chemical bonding between the hydroxyl groups of graphene with polyurethane. These nanocomposites exhibited enhanced mechanical and thermal properties, in addition to good shape recovery in relation to the neat polymer. The addition of 2 wt% of the functionalized graphene nanoplatelets showed that the Young's modulus and the thermal stability (at 30 °C) were ten times higher compared to a pure PU.

Graphene can be produced by unzipping multi-walled carbon nanotubes (MWCNT), which is called graphene nanoribbons (GNRs) (Lian et al. 2014). Lian et al. (2014) prepared GNRs by the CNT unzipping method, which were functionalized with non-covalent groups. These nanoparticles were used as reinforcement nanofillers for poly(vinyl chloride) (*PVC*) and poly(methyl methacrylate) (*PMMA*). GNRs were better dispersed in the PVC and PMMA matrices after the surface modification and exhibited strong interaction with matrices. The mechanical properties of both PVC and PMMA were enhanced. The effect of the addition of functionalized GNRs is most often superior to the addition of pure GNRs, or of functionalized carbon nanotubes or even of pure carbon nanotubes.

1.1.4.3 Electrical Applications

Some studies on graphene are related to mechanical reinforcement. However, the great majority of graphene composite applications are in the field of nanoelectronics. Despite all the exceptional properties mentioned in the previous chapters, graphene possesses zero band gap and chemical inertia. This characteristic limits the graphene applications as semiconductors and sensors. The surface modification by functionalization, both covalent and non-covalent, can modify the electronic properties of graphene by opening the energy gap, making possible nanoelectronic device applications (Georgakilas et al. 2012; Boukhvalov and Katsnelson 2009). The creation of this bang gap has driven many researches and has generated innovative applications in digital electronics, infrared nanophotonics, pseudospintronics, and terahertz technology (Xia et al. 2010).

Nowadays, new methods of energy conversion and storage have been developed, but the low efficient of these methods is an issue to be overcome. Therefore, much attention is given to the development of supercapacitors. Supercapacitors are energy storage devices capable of providing high power density by electrochemical systems. The energy conversion/storage capacity is dependent on the electrostatic forces between the electrode/electrolyte interface (Huang et al. 2013; Yu et al. 2014). Ren et al. (2015) functionalized rGO with methyl green (MG), obtaining a non-covalent functionalization and enhancing the supercapacitive performance. The

mass ratio of 5:4 for the composite (rGO:MG) achieved a specific capacitance as high as 341 F g^{-1} at Ag^{-1} in the potential range of −0.25 to 0.75 V. The functionalization of rGO with MG provided an enhancement of 180 % in the specific capacitance when compared with pure RGO. These results showed that the functionalization of GO is an effective way to make new electrode materials, especially for supercapacitor systems.

When it comes to new technologies for energy generation and storage, many studies have also focused on the functionalized graphene applied in photovoltaic devices, such as solar cells. Graphene has been used in the development of organic solar cells, quantum dot solar cells (Chen et al. 2011), and dye-sensitized solar cells, among others (Wan et al. 2011), due to its favorable properties, such as high transparency in the visible spectrum and weak changes in electrical conductance (Lim et al. 2015; Wan et al. 2011; Liu et al. 2008).

Organic photovoltaic (OPV) cells produced with conjugated polymers have the advantages of low cost, solution-based processing, and fabrication on a flexible substrate. Due to these advantages, OPV cells have attracted much interest in solar cells technology. One of the goals in the field of solar cells is to increase significantly the power conversion efficiency (PCE). New processing techniques and new materials must be developed to achieve this objective. Graphene has demonstrated many advantages when compared with traditional transparent electrodes, thanks to its exceptional electrical properties, high mobility, and facility to change the surface by functionalization treatments (Wan et al. 2011; Liu et al. 2008; Yu et al. 2011). Lim et al. (2015) investigated the effects of surface-treated graphene thin films on the performance of organic solar cells for different surface treatments: (i) annealing in argon ambient, (ii) dipping in acetone, (iii) ultraviolet irradiation, and (iv) nitrogen plasma treatment. Organic solar cells were made with graphene and indium/tin oxide electrodes. The results showed that the device made with graphene and treated with acetone presented the best performance, including a better PCE value when compared with solar cell without graphene and cell with another surface-treated graphene. The authors concluded that the addition of acetone-modified graphene is very simple and can be used for other types of solar cells.

Graphene is an exceptional material for the detection of gases, ions, and biomolecules. Therefore, the functionalized graphene is the most promising nanomaterial for sensor fabrication. Besides the high surface area, graphene can also change its conductance due to molecule adsorption on its surface. This property makes graphene sensitive to many different molecules. For the most part, graphene is widely used in sensing applications in the biotechnology field, especially for the detection of diseases and biomolecules. Many researchers found that the functionalized graphene combined with single-stranded DNA and fluorescent molecules can diagnose several diseases. Fluorescent molecules are attached to the DNA, and then, they attached to graphene. This system is capable of detecting glucose, NADH, cholesterol, hydrogen peroxide, and others (Kuila et al. 2012). One example of this application is shown by Yang et al. (2015). They prepared a versatile nanocomposite with β-cyclodextrin functionalized graphene (CD-GR) with grafted fragments of DNA on the CD-GR surface to create a modified

electrode which worked as a DNA biosensor. Due to the high surface area of graphene and the multi-site characteristic of CD, they concluded that the hybridization kinetics and biosensor efficiency were improved: The biosensor demonstrated a low background response and extremely high sensitivity for target DNA.

Du et al. (2015) also developed a biosensor based on the functionalized graphene. They deposited gold nanostructure on reduced graphene oxide that was functionalized for glucose sensing. The functionalization was made with β-lactoglobulin. The biosensor exhibits remarkable sensitivity and rapid response time, showing that the performance of the fabricated sensor is suitable for quantitative detection of glucose. Shen et al. (2015) synthesized a new aldehyde-functionalized graphene nanocomposite with poly-(epichlorohydrin) and 4-pyridinecarboxaldehydea for electrochemical immunosensor for identifying cancer. The aldehyde–functionalized graphene nanocomposite provided a promising method to immobilize and capture the antibodies on the electrode surface.

1.1.4.4 Anti-corrosion Applications

In addition to the electrical and mechanical applications, graphene is also being used to enhance the tribological and anti-corrosion properties of polymers, since it can inhibit corrosion and increase the polymer resistance.

Liu et al. (2015d) produced nanocomposites with two different fillers, functionalized fullerene C_{60} (FC_{60}) and functionalized graphene (FG) using a polymer matrix of epoxy coating, and studied the tribological and anti-corrosion performances of these materials. They showed that the addition of FC_{60} and FG into epoxy matrix greatly improved the tribological and anti-corrosion properties when compared to the pure epoxy, which occurs due to the lubrication and barrier properties of nanofillers. The difference between the structure of fullerene and graphene results in their unique tribological properties. FC_{60} presented better tribological and scratch resistance, while FG showed better anti-corrosion performance. The authors concluded that the properties of epoxy nanocomposite depended on the nanofillers shape, and they also concluded that the functionalized graphene can be used for anti-corrosion applications.

Tribological and anti-corrosion properties have been studied not only with epoxy nanocomposites, but also with other polymer matrices as well. Mo et al. (2015) functionalized graphene (graphene named FG) and graphene oxide (graphene named FGO) with 3-aminopropyltriethoxysilane (APTES), and fabricated a series of polyurethane (PU)-based nanocomposites reinforced with different contents of FG and FGO. The tribological and anti-corrosion mechanisms of polyurethane nanocomposite were analyzed. They observed better dispersion and compatibility after the functionalization. Both FG and FGO addition enhanced the tribological and anti-corrosion properties, due to the lubrication and barrier properties provided by the addition. When the authors compared FG/PU with FGO/PU nanocomposites, FGO exhibited better tribological property but FG presented a better anti-corrosion

property. As in the work cited in the previous paragraph, in this case, the addition of graphene in a polymer matrix was also able to improve the corrosion resistance of the material.

The functionalized graphenes have been extensively used in different areas of science. Many researches have conducted studies that incorporate the functionalized graphene in nanoelectronic devices, and biosensor systems, such as mechanical and anti-corrosion reinforcement, among other areas. Due to its exceptional properties, many other applications have been developed. It is necessary to innovate in order to achieve the best qualities of the material for the most promising applications.

1.1.5 Characterization of Functionalized Graphene

1.1.5.1 Raman Spectroscopy

Raman spectroscopy is a technique used to analyze geometric structure and chemical bonding of molecules. This aspect makes Raman spectroscopy extremely useful in studies of different allotropes of carbon, such as diamond, fullerenes, carbon nanotubes, graphene, and functionalized graphene. A typical Raman spectrum of carbon materials, including graphene, shows the presence of two prominent peaks, known as D and G bands. The G band is located at 1500–1590 cm^{-1} and is associated with disordered samples or edges (sp^3 carbon domains). The D band is at 1290–1350 cm^{-1} and corresponds to graphitic domain (sp^2 carbon domains). Graphene has an additional peak around 2700 cm^{-1}, which is known as G′, sometimes referred as an overtone of the D band. This band is used to determine the graphene layer thickness (Zhang et al. 2012a; Xue et al. 2015; Lin et al. 2015) (Fig. 1.9).

The D band intensity is higher when the presence of defects and impurities increases, as observed in Fig. 1.9. Graphene oxides (GO) have some natural functional groups, showing a more intense D band when compared to graphite and graphene. The 2D band is highly sensitive to the number of graphene layers. When few layers of graphene are compared to graphene oxide, the 2D band intensity is attenuated and its bandwidth is broader. The functional groups in graphene oxide are able to stack large number of graphene layers (Maktedar et al. 2014; Feng et al. 2012; Kudin et al. 2007).

The intensity ratio of D band over G band (I_D/I_G) is usually used to investigate the amount of structural defect and disorder. Some defects may occur due to the use of catalysts during its synthesis or due to the attachment of functional groups on the graphene surface. The I_D/I_G ratio is proportional to the number of defects or changes on graphene layer. Table 1.2 shows I_D/I_G of different functionalized graphene forms (Malard et al. 2009; Mhamane et al. 2011; Liu et al. 2014).

Table 1.2 shows that the I_D/I_G ratio increases with the graphene functionalization when compared to few layers of graphene or graphite. This can be assigned to the formation of covalent or non-covalent bonds between the functional groups and the graphene surfaces (Kaur et al. 2015).

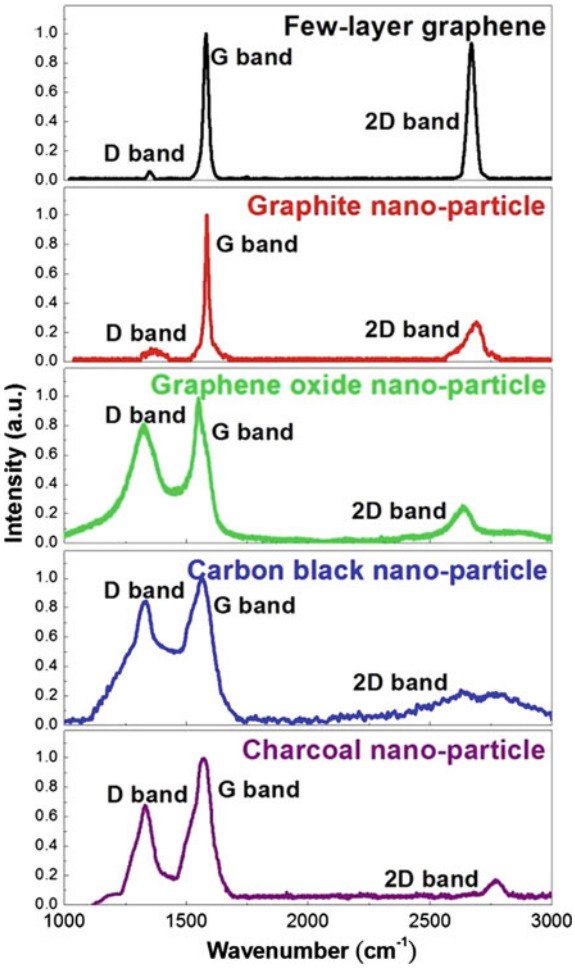

Fig. 1.9 The Raman scattering spectra of few-layer graphene, graphite nanoparticle, graphene oxide nanoparticle, carbon black nanoparticle, and charcoal nanoparticle. (Adapted from Lin et al. 2015)

Table 1.2 I_D/I_G ratio of different graphene functionalization

Functionalization Type	I_D/I_G ratio	References
Few-layer graphene	0.06	Lin et al. (2015)
Graphite nanoparticle	0.08	Lin et al. (2015)
Graphene oxide	0.8–1.018	Lin et al. (2015), Xue et al. (2015), Mhamane et al. (2011)
Graphene oxide ethylenediamine	1.10–1.15	Xue et al. (2015)
Graphene–poly(diallyl dimethylammonium) chloride	1.057	Kaur et al. (2015)
Fluorinated graphene oxide	0.75–0.85	Park and Lee (2016)
Graphene–diazonium	1.42	Liu et al. (2014)

1.1.5.2 X-ray Diffraction (XRD)

X-ray diffraction technique is used to determine the presence of functional groups on the graphene surface. A typical XRD pattern of graphite shows an intense and sharp peak at around 2θ = 26°, referring to the plane (002) of the graphene sheet. After a chemical modification of graphite by the Hummers' method to obtain the graphene oxide, that peak is shifted to around 10° (2θ). GO can be reduced by thermal or chemical treatments to reduced graphene oxide (rGO). The XRD of rGO shows a narrow peak at around 24° (Fig. 1.10). These peak shifts suggest full oxidation and efficient formation of well-ordered two-dimensional structures of graphene sheets after the reduction of GO to rGO (Cui et al. 2011; Park and Lee 2015; Dreyer et al. 2009).

Other expressive changes can be observed in the interlayer distances between the aromatic rings of graphene sheets. This distance can be determined by the following expression:

$$d_{(002)} = \frac{n\lambda}{2\text{sen}\theta} \tag{1.1}$$

where n is order of reflection equal to 1, λ is the wavelength of cooper irradiation equal to 0.154 nm, $d_{(002)}$ is the interplanar distance between graphene sheets, and 2θ is the diffraction angle. The values of $d_{(002)}$ obtained in Fig. 1.10 were 0.334, 0.86, and 0.368 nm for graphite, graphene oxide, and reduced graphene, respectively. The increase in the $d_{(002)}$ value of graphene oxide is related to the insertion of functional groups (epoxy, hydroxyl, and carboxyl) between the graphene sheets.

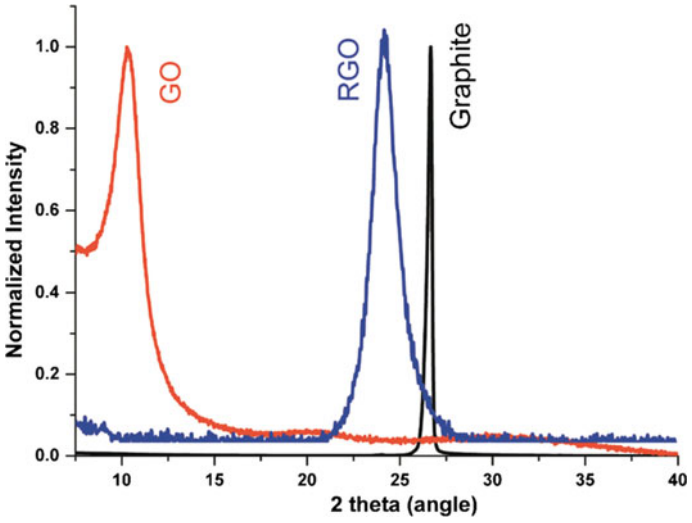

Fig. 1.10 XRD pattern of graphite (*black*), graphene (*red*), and reduced graphene oxide (*blue*) (Cui et al. 2011)

Table 1.3 $d_{(002)}$ and 2θ values of different graphene functionalizations

Functionalization type	$d_{(002)}$	2θ	References
Graphite	0.334	26.7°	Cui et al. (2011), Su et al. (2016)
Graphene	0.368	24.16°	Cui et al. (2011)
Graphene oxide	0.856–0.86	10.27–10.32°	Cui et al. (2011), Su et al. (2016)
Reduced graphene-NH_2	–	23.05°	Su et al. (2016)
Reduced graphene-liquid crystalline polymer (LCP)	1.09–1.18 nm	10.17–7.58°	Ji et al. (2015)
Reduced graphene-amine-terminated polyether	Significant enlargement in interlayer spacing	<5°	Qian et al. (2014)
Reduced graphene with *p*-phenylenediamine	0.352	24.8°	Lu et al. (2015)
Graphene oxide with *p*-phenylenediamine	1.348	6.5°	Lu et al. (2015)
Fluorinated graphene oxide	0.771–0.830	10.65–11.47°	Park and Lee (2016)

After the reduction of graphene oxide, the $d_{(002)}$ value is close to that of the graphite, suggesting an efficient bond removal of the graphene layer. Other shifts in the $d_{(002)}$ value can be observed when the graphene is subject to other types of functionalization agent. Table 1.3 lists the $d_{(002)}$ and 2θ values after graphene functionalization. The intercalation of different molecules in the graphene sheets significantly changes these parameters (Ji et al. 2015; Qian et al. 2014).

1.1.5.3 Fourier Transform Infrared Spectroscopy Analysis (FTIR)

Fourier transform infrared spectroscopy is used to study the chemical constituents of graphene after surface modification. Figure 1.11 shows a typical FTIR spectrum of graphene oxide obtained by the Hummers' method.

The peaks at 1740 and 1370 cm^{-1} are due to C=O and C–O stretching vibration, respectively. Figure 1.11 shows peaks at 1220, 880, and 850 cm^{-1} related to the presence of symmetric stretching, asymmetric stretching, and deformation vibrations of epoxy groups, respectively. Finally, Fig. 1.11 shows the peak at around 3390 cm^{-1}, which is related to O-H stretching vibration of adsorbed water molecules (Oh et al. 2010; Lu et al. 2015; Naebe et al. 2014; Marcano et al. 2010). Table 1.4 shows the appearance of some bands associated with many treatments. The presence of these chemical groups is able to promote significant improvements in the graphene properties, such as solubility, thermal, electrical, and mechanical capacities (Naeimi et al. 2016).

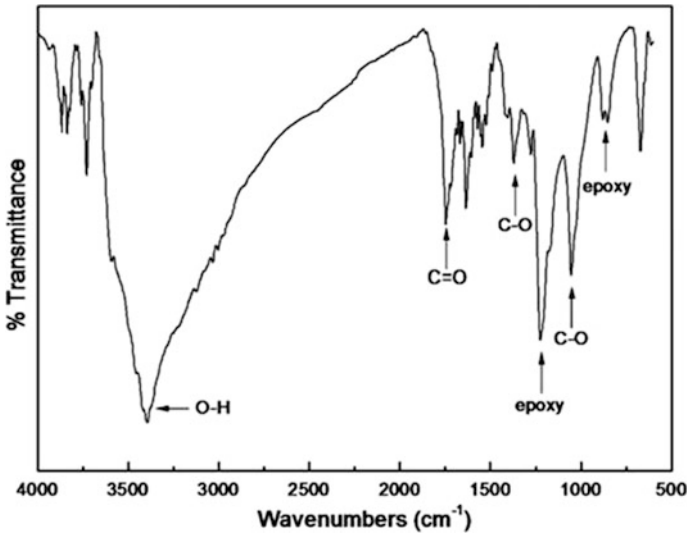

Fig. 1.11 The FT-IR spectrum of graphene oxide (Oh et al. 2010)

Table 1.4 Peak identification of FTIR spectra of graphenes subject to different treatments

Functionalization method	Wavenumber (cm^{-1})	Assignment	References
Reduced graphene with Bingel reaction	1731	C=O stretch	Naebe et al. (2014)
Graphene oxide with *p*-phenylenediamine	1265	C–N stretch	Lu et al. (2015)
	810	N–H wag	
Reduced graphene with *p*-phenylenediamine	1515	N–H bending	Lu et al. (2015)
	1265	C–N stretch	
	810	N–H wag	
Graphene oxide with amine-terminated polyether	1564	N–H stretch	Qian et al.
	1010	C–O–C stretch	
Reduced graphene with *p*-phenylenediamine and isoamyl nitrite	1380	C–N stretch	Liu et al. (2013)
Graphene oxide with fluorine–nitrogen gases	1100	C–F stretch	Park and Lee (2016)
Graphene oxide with diethylenetriamine	3440	N–H stretch	Su et al. (2016)
	1201	C–N stretch	

1.1.5.4 Thermogravimetric Analysis (TGA)

TGA is a valuable and fairly simple method for investigating thermal stability, as well as for analyzing the presence of functional group in carbonaceous materials. Large differences related to mass loss can be observed when graphene is compared with the functionalized graphene. Figure 1.12 shows the TGA of graphene oxide (GO) and reduced graphene produced via γ-ray induced graphene oxide (rGO) (Zhang et al. 2012b).

The mass loss of GO is 5 % at around 100 °C, which can be assigned to the removal of water molecules trapped inside the GO structure. At around 200 °C, with mass loss of 31 %, the pyrolysis of the labile oxygen-containing groups occurs until the formation of CO, CO_2, and steam. The TGA of rGO shows a mass loss between 130 and 250 °C due to the decomposition of residual oxygen-containing groups. Therefore, γ-ray induced reduction (forming rGO), but also improves the thermal stability when compared with GO. Maktedar et al. (2014) functionalized reduced graphene oxide with 6-aminoindazole (6-AIND). The TGA results showed that graphene oxide presented a total of 82.9 % in mass loss due to the removal of thermally labile oxygen-containing groups. Meanwhile, reduced graphene oxide–6-AIND presented a total loss of 40.9 %, suggesting its thermal stability is higher than graphene oxide. The reduced mass loss of reduced graphene oxide–6-AIND and the enhanced residues formation depicts the high interaction between graphene and the new functional groups. Naeimi et al. (2016) prepared sulfonated graphene and predicted the amount of functional groups per carbon atoms through TGA analysis. For that purpose, weight loss values were employed together with the molecular weight of the various groups, according to Eq. (2):

$$X = \frac{R(\%) \cdot M_W(\mathrm{g/mol})}{L(\%) \cdot 12(\mathrm{g/mol})} \tag{2}$$

where X stands for the number of carbon atoms in sulfonated graphene nanosheets per each covalent functional group, R (%) is the remaining mass in the TGA, L (%)

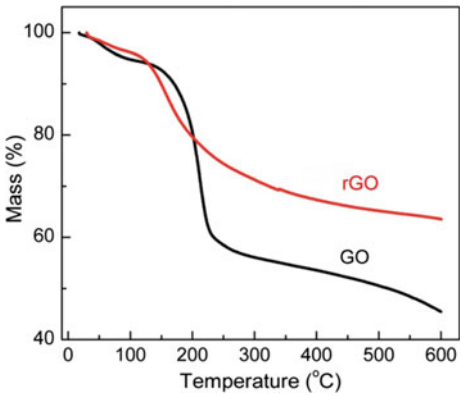

Fig. 1.12 TGA curves of graphene oxide (GO) and γ-ray induced graphene oxide (rGO) (Zhang et al. 2012b)

is the weight loss range, and molecular weight (M_w) is the weight of the sulfonated groups. For that study, X was equal to 34 carbon atoms, which represents one functionalization group for approximately 34 carbon atoms.

1.1.5.5 X-ray Photoelectron Spectroscopy (XPS)

X-ray photoelectron spectroscopy (XPS) is one of the most sensitive and informative surface analysis techniques available. XPS analysis can be used on graphene materials to determine the functionalization degree. Marcano et al. (2010) developed three different graphene oxides using the Hummers' method (HGO), improved Hummers' method (IGO), and modified Hummers' method (HGO^+). The XPS spectrum was able to determine the relative levels of oxidation (Fig. 1.13).

The spectra of the samples in Fig. 1.13 show that IGO is the most oxidized material and that IGO has a more organized structure than the other two materials. Using deconvolution, the peaks of all samples can be split into four peaks that correspond to the following groups: carbon sp^2 (C=C, 284.8 eV), epoxy/hydroxyls (C–O, 286.2 eV), and carboxylates (O–C = O, 289.0 eV). The percentages of oxidized carbon and graphitic carbon in the IGO sample were 69 and 31 %, respectively. The HGO^+ sample presented 63 and 37 %, while HGO contained 61 and 39 % of oxidized carbon and graphitic carbon, respectively. This suggests that XPS technique can accurately detect different levels of functionalization on graphene.

1.1.5.6 Dispersion of Functionalized Graphene in Different Solvents

The processability of aqueous graphene dispersions has attracted significant attention in various applications, including flexible electronics, batteries, conductive paper, and wire fabrications. Many studies were developed in order to achieve

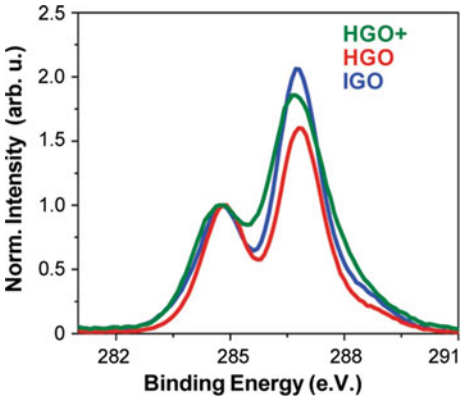

Fig. 1.13 C1s XPS spectra of improved Hummers' method (IGO), Hummers' method (HGO), and modified Hummers' method (HGO^+) (Marcano et al. 2010)

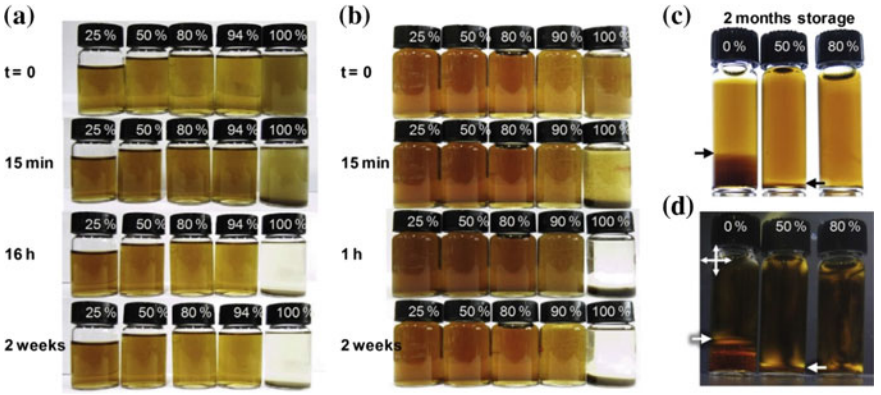

Fig. 1.14 Stability of the graphene oxide dispersions in organic binary solvents: **a** water/methanol, **b** water/dioxane, and **c**–**d** water/dioxane without and with crossed polarizers. The numbers on the top denote the concentration of organic solvent (Ahmad et al. 2016)

stable dispersions in various solvents such as water, dimethylformamide, alcohol, acetone, tetrahydrofuran, glycols, and alkanes (Zhang et al. 2012b; Ahmad et al. 2016). Graphene functionalization is one way of accomplishing successful dispersion in different solvents. Ahmad et al. (2016) introduced a new approach to enhance the graphene oxide dispersity in immiscible solvents. They prepared graphene oxide dispersions by mixing water/methanol and water/dioxane binary solvents. The results showed (Fig. 1.14) that the graphene oxide dispersion in 100 % methanol and 100 % dioxane exhibited poor stability. However, dispersions in the binary solvents (water/methanol and water/dioxane) exhibited excellent dispersivity. In these cases, the graphene oxide dispersity was even better than in pure water and no sedimentation was observed. Water molecules in these binary dispersions act like a surfactant. These molecules are located primarily around the graphene oxide particles, resulting in the separation of the graphene oxide sheets (Konios et al. 2014; Ahmad et al. 2016). Therefore, the dispersion of graphene in different solvents can also be used as a characterization method for their functionalization.

References

Ahmad RTM, Hong SH, Shen TZ et al (2016) Water-assisted stable dispersal of graphene oxide in non-dispersible solvents and skin formation on the GO dispersion. Carbon 98:188–194

Allen MJ, Tung VC, Kaner RB (2010) Honeycomb carbon: a review of graphene. Chem Rev 110:132–145

Besenhard JO (1976) The electrochemical preparation and properties of ionic alkali metaland NR4-graphite intercalation compounds in organic eletrolytes. Carbon 14:111–115
Boehm HP, Clauss A, Fischer G et al (1962) Surface properties of extremely thin graphite lamellae. In: Proceedings of the fifth conference on carbon, p 73
Bose S, Kuila T, Kim NH et al (2014) Graphene produced by electrochemical exfoliation. Woodhead Publishing Limited, pp 81–98
Boukhvalov DW, Katsnelson MI (2009) Chemical functionalization of graphene. J Phys Condens Matter 21:344205
Cai D, Yang D, Wang D et al (2015) Tin dioxide dodecahedral nanocrystals anchored on graphene sheets with enhanced electrochemical performance for lithium-ion batteries. Electrochim Acta 159:46–51
Çelebi C, Yanık C, Demirkol AG et al (2012) The effect of a SiC cap on the growth of epitaxial graphene on SiC in ultra-high vacuum. Carbon 50:3026–3031
Chatterjee SG, Chatterjee S, Ray AK et al (2015) Graphene-metal oxide nanohybrids for toxic gas sensor: a review. Sens Actuators B 221:1170–1181
Chen J, Li C, Eda G et al (2011) Incorporation of graphene in quantum dot sensitized solar cells based on ZnO nanorods. Chem Commun (Cambrigde, England) 47:6084–6086
Chen C, Ru Q, Hu S et al (2015) Co_2SnO_4 nanocrystals anchored on graphene sheets as high-performance electrodes for lithium-ion batteries. Electrochim Acta 151:203–213
Chia JSY, Tan MTT, Khiew PS et al (2015) A bio-electrochemical sensing platform for glucose based on irreversible, non-covalent pi–pi functionalization of graphene produced via a novel, green synthesis metho. Sens Actuators B 210:558–565
Choi BG, Park H, Yang MH et al (2010) Microwave-assisted synthesis of highly water-soluble graphene towards electrical DNA sensor. Nanoscale 2:2692–2697
Compton OC, Jain B, Dikin DA et al (2011) Chemically active reduced graphene oxide with tunable C/O ratios. ACS Nano 5:4380–4391
Coraux J, N'Diaye AT, Busse C et al (2008) Structural coherency of graphene on Ir(111). Nano Lett 8:565–570
Cui P, Lee J, Hwang E et al (2011) One-pot reduction of graphene oxide at subzero temperatures. Chem Commun 47:12370–12372
Dong XC, Xu H, Wang XW et al (2012) 3D graphene–cobalt oxide electrode for highperformance supercapacitor and enzymeless glucose detection. ACS Nano 6:3206–3213
Dreyer DR, Park S, Bielawski CW et al (2009) The chemistry of graphene oxide. Chem Soc Rev 39:228–240
Du X, Zhang Z, Miao Z et al (2015) One step electrodeposition of dendritic gold nanostructures on β-lactoglobulin-functionalized reduced graphene oxide for glucose sensing. Talanta 144:823–829
Elías AL, Méndez ARB, Rodríguez DM et al (2010) Longitudinal cutting of pure and doped carbon nanotubes to form graphitic nanoribbons using metal clusters as nanoscalpels. Nano Lett 10:366–372
Feng SY, Ma JJ, Lin XY et al (2012) Covalent functionalization of graphene oxide by 9-(4-aminophenyl) acridine and its derivatives. Chinese Chem Lett 23:1411–1414
Ferreira FV, Francisco W, Menezes BRC et al (2015) Carbon nanotube functionalized with dodecylamine for the effective dispersion in solvents. Appl Surf Sci 357:2154–2159
Frank O, Kalbac M (2014) Chemical vapor deposition (CVD) growth of graphene films. Woodhead Publishing Limited, pp 27–49
Geim AK, Novoselov KS (2007) The rise of graphene. Nat Mater 6:183–191
Georgakilas V, Otyepka M, Bourlinos AB et al (2012) Functionalization of graphene: covalent and non-covalent approaches, derivates and applications. Chem Rev 112:6156–6214
Goenka S, Sant V, Sant S (2014) Graphene-based nanomaterials for drug delivery and tissue engineering. J Controlled Release 173:75–88
Grachova Y, Vollebregt S, Lacaita AL et al (2014) High quality wafer-scale CVD graphene on molybdenum thin film for sensing application. Procedia Eng 87:1501–1504

Green AA, Hersam MC (2009) Graphene and its derivatives for cell biotechnology. Analyst 9:4031–4036
Haldar S, Bhandary S, Bhattacharjee S et al (2012) Functionalization of edge reconstructed graphene nanoribbons by H and Fe: a density functional study. Solid State Commun 152:1719–1724
Han MY, Özyilmaz B, Zhang Y et al (2007) Energy band-gap engineering of graphene nanoribbons. Phys Rev Lett 98:206805
Hassan HMA, Abdelsayed V, Khder AERS et al (2015) Microwave synthesis of graphene sheets supporting metal nanocrystals in aqueous and organic media. J Mater Chem 19:3832–3837
Hirsch A (2009) Unzipping carbon nanotubes: a peeling method for the formation of graphene nanoribbons. Angew Chem Int 6594–6596
Ho CY, Wang HW (2015) Characteristics of thermally reduced graphene oxide and applied for dye-sensitized solar cell counter electrode. Appl Surf 357:147–154
Hossain MZ, Johns JE, Bevan KH et al (2012) Chemically homogeneous and thermally reversible oxidation of epitaxial graphene. Nat Chem 4:305–309
Huang Z, Zhang H, Chen Y et al (2013) Microwave-assisted synthesis of functionalized graphene on Ni foam as electrodes for supercapacitor application. Electroc Acta 108:421–428
Hummers WS, Offeman RE (1958) Preparation of graphitic oxide. J Am Chem Soc 80:1339
Jayasena B, Melkote SN (2015) An investigation of PDMS stamp assisted mechanical exfoliation of large area graphene. Procedia Manuf 1:840–853
Ji Liangliang, Yanhong Wu, Ma Lijun et al (2015) Noncovalent functionalization of graphene with pyrene-terminated liquid crystalline polymer. Compos Part A Appl 72:32–39
Jiao L, Zhang L, Wang X et al (2009) Narrow graphene nanoribbons from carbon nanotubes. Nature 458:877
Jo S, Park YH, Ha SG et al (2015) Simple noncovalent hybridization of polyaniline with graphene and its application for pseudocapacitor. Synthetic Met 209:60–67
Karamat S, Sonuşen S, Çelikd U et al (2015) Synthesis of few layer single crystal graphene grains on platinum by chemical vapour deposition. Prog Nat Sci Mater Inter 25:291–299
Kaur P, Shin MS, Sharma S et al (2015) Non-covalent functionalization of graphene with poly (diallyl dimethylammonium) chloride: effect of a non-ionic surfactant. Int J Hydrogen Energ 40:1541–1547
Kim JY, Grossman JC (2015) High-efficiency thermoelectrics with functionalized graphene. Nano Lett 15:2830–2835
Kim H, Abdala AA, Macosko CW (2010) Graphene/polymer nanocomposites. Macromolecules 43:6515–6530
Kim JY, Lee JH, Grossman (2012) Thermal transport in functionalized graphene. ACS Nano 6:9050–9057
Konios D, Stylianakis MM, Stratakis E et al (2014) Dispersion behaviour of graphene oxide and reduced graphene oxide. J Colloid Interf Sci 430:108–112
Kosynkin DV, Higginbotham AL, Sinitskii A et al (2009) Longitudinal unzipping of carbon nanotubes to form graphene nanoribbons. Nature 458:872
Kudin KN, Ozbas B, Schniepp HC et al (2007) Raman spectra of graphite oxide and functionalized graphene sheets. Nano Lett 8:36–41
Kuila T, Bose S, Mishra AK et al (2012) Chemical functionalization of graphene and its applications. Prog Mat Sci 57:1061–1105
Kumar B, Baraket M, Paillet M et al (2016) Growth protocols and characterization of epitaxial graphene on SiC elaborated in a graphite enclosure. Phys E (Amsterdam, Neth.) 75: 7–14
Layek RK, Nandi AK (2013) A review on synthesis and properties of polymer functionalized graphene. Polymer 54:5087–5103
Li L, Qin R, Li H et al (2011) Functionalized graphene for high-performance two-dimensional spintronics devices. ACS Nano 5:2601–2610
Li Y, Peng Z, Larios E et al (2015) Rebar graphene from functionalized boron nitride nanotubes. ACS Nano 9:532–538

Lian M, Fan J, Shi Z et al (2014) Kevlar®-functionalized graphene nanoribbon for polymer reinforcement. Polymer (United Kingdom) 55:2478–2587
Liao L, Peng H, Liu Z (2014) Chemistry makes graphene beyond graphene. J Am Chem Soc 136:12194–12200
Lim T, Su C, Song M et al (2015) Organic solar cells with surface-treated graphene thin fi lm as interfacial layer. Synthet Metals 205:1–5
Lin Z, Liu Y, Yao Y et al (2011) Superior capacitance of functionalized graphene. J Phys Chem 115:7120–7125
Lin YH, Yang CY, Lin SF et al (2015) Triturating versatile carbon materials as saturable absorptive nano powders for ultrafast pulsating of erbium-doped fiber lasers. Opt Mat Expr 5:236–253
Liu Z, Liu Q, Huang Y et al (2008) Organic photovoltaic devices based on a novel acceptor material: Graphene. Adv Mat 20:3924–3930
Liu H, Ryu S, Chen Z et al (2009) Photochemical reactivity of graphene. J Am Chem Soc 131:17099–17101
Liu M, Duan Y, Wang Y et al (2014) Diazonium functionalization of graphene nanosheets and impact response of aniline modified graphene/bismaleimide nanocomposites. Mater Design 53:466–474
Liu H, Kishi N, Soga T (2015a) Synthesis of thiolated few-layered graphene by thermal chemical vapor deposition using solid precursor. Mat Lett 159:114–117
Liu J, Liu Z, Barrow CJ et al (2015b) Molecularly engineered graphene surfaces for sensing applications: a review. Anal Chim Acta 859:1–19
Liu D, Zhao W. Liu S et al (2015c) Comparative tribological and corrosion resistance properties of epoxy composite coatings reinforced with functionalized fullerene C60 and graphene. Surf Coat Technol 286:354–364
Liu L, Qing M, Wang Y et al (2015d) Defects in graphene: generation, healing, and their effects on the properties of graphene: a review. J Mater Sci Technol 31:599–606
Liu X, Han Y, Evans JW et al (2015e) Growth morphology and properties of metals on graphene. Prog Surf Sci 90:397–443
Lu X, Li L, Song B et al (2015) Mechanistic investigation of the graphene functionalization using p-phenylenediamine and its application for supercapacitors. Nano Energy 17:160–170
Lv W, Li Z, Deng Y et al (2015) Graphene-based materials for electrochemical energy storage devices: opportunities and challenges. Energy Storage Mater (in press)
Maktedar SS, Mehetre SS, Singh M et al (2014) Ultrasound irradiation: a robust approach for direct functionalization of graphene oxide with thermal and antimicrobial aspects. Ultrason Sonochem 21:1407–1416
Malard LM, Pimenta MA, Dresselhaus G et al (2009) Raman spectroscopy in graphene. Phys Rep 473:51–87
Mao HY, Lu YH, Lin JD et al (2013) Manipulating the electronic and chemical properties of graphene via molecular functionalization. Prog Surf Sci 88:132–159
Marcano DC, Kosynkin DV, Berlin JM et al (2010) Improved synthesis of graphene oxide. ASCNANO 4:4806–4814
Márquez AGC, Macías FJR, Delgado JC et al (2009) Ex-MWCNTs: graphene sheets and ribbons produced by lithium intercalation and exfoliation of carbon nanotubes. Nano Lett 9:1527–1533
Mhamane D, Ramadan W, Fawzy M et al (2011) From graphite oxide to highly water dispersible functionalized graphene by single step plant extract-induced deoxygenation. Green Chem 13:1990–1996
Mittal G, Dhand V, Rhee KY et al (2015) A review on carbon nanotubes and graphene as fillers in reinforced polymer nanocomposites. J Ind Eng Chem 21:11–25
Mo M, Zhao W, Chen Z et al (2015) Excellent tribological and anti-corrosion performance of polyurethane composite coatings reinforced with functionalized graphene and graphene oxide nanosheets. RSC Adv 5:56486–56497

Mohanty N, Berry V (2008) Graphene-based single-bacterium resolution biodevice and DNA transistor: interfacing graphene derivatives with nanoscale and microscale biocomponents. Nano Lett 8:4469–4476
Naebe M, Wang J, Amini A et al (2014) Mechanical property and structure of covalent functionalised graphene/epoxy nanocomposites. Sci Rep 4:1–7
Naeimi H, Golestanzadeh M, Zahraie Z et al (2016) Synthesis of potential antioxidants by synergy of ultrasound and acidic graphene nanosheets as catalyst in water. Int J Biol Macromol 83:345–357
Niyogi S, Bekyarova E, Itkis ME et al (2010) Spectroscopy of covalently functionalized graphene. Nano Lett 10:4061–4066
Novoselov KS, Geim AK, Morozov SV et al (2004) Electric field effect in atomically thin carbon films. Science 306:666–669
Oh J, Lee JH, Koo JC et al (2010) Graphene oxide porous paper from amine-functionalized poly (glycidyl methacrylate)/graphene oxide core-shell microspheres. J Mater Chem 20:9200–9204
Oznuluer T, Pince E, Polat OA et al (2011) Synthesis of graphene on gold. Appl Phys Lett 98:183101
Park MS, Lee YS (2016) Functionalization of graphene oxide by fluorination and its characteristics. J Fluorine Chem 182:91–97
Parvez K, Yang S, Feng X et al (2015) Exfoliation of graphene via wet chemical routes. Synth Met (in press)
Pinto AM, Gonçalves IC, Magalhães FD (2013) Graphene-based materials biocompatibility: a review. Colloids Surf B 111:188–202
Qian X, Song L, Yu B et al (2014) One-pot surface functionalization and reduction of graphene oxide with long-chain molecules: preparation and its enhancement on the thermal and mechanical properties of polyuria. Chem Eng J 236:233–241
Ren X, Hu Z, Hu H et al (2015) Noncovalently-functionalized reduced graphene oxide sheets by water-soluble methyl green for supercapacitor application. Mat Resear Bull 70:215–221
Renteria J, Legedza S, Salgado R et al (2015) Magnetically-functionalized self-aligning graphene fillers for high-efficiency thermal management applications. Mater Des 88:214–221
Rohini R, Katti P, Bose S (2015) Tailoring the interface in graphene/thermoset polymer composites: a critical review. Polymer 70:A17–A34
Sanchez VC, Jachak A, Hurt RH et al (2012) Biological interactions of graphene-family nanomaterials: an interdisciplinary review. Chem Res Toxicol 25:15–34
Sayin CS, Toffoli D, Ustunel H (2015) Covalent and noncovalent functionalization of pristine and defective graphene by cyclohexane and dehydrogenated derivatives. App Surf Sci 351:344–352
Shen G, Zhang X, Shen Y et al (2015) Immobilization of antibodies on aldehyde-functionalized polymer/graphene films for the fabrication of a label-free electrochemical immunosensor. J Electroanal Chem 759:67–71
Shin HJ, Kim KK, Benayad A et al (2009) Efficient reduction of graphite oxide by sodium borohydride and its effect on electrical conductance. Adv Funct Mater 19:1987–1992
Singh V, Joung D, Zhai L et al (2011) Graphene based materials: past, present and future. Prog Mater Sci 56:1178–1271
Somani PR, Somani SP, Umeno M (2006) Planer nano-graphenes from camphor by CVD. Chem Phys Lett 430:56–59
Song Y, He Z, Hou H et al (2012) Architecture of Fe3O4–graphene oxide nanocomposite and its application as a platform for amino acid biosensing. Electrochim Acta 71:58–65
Stankovich S, Dikin DA, Piner RD et al (2007) Synthesis of graphene-based nanosheets via chemical reduction of exfoliated graphite oxide. Carbon 45:1558–1565
Su Z, Wang H, Tian K et al (2016) Simultaneous reduction and surface functionalization of graphene oxide with wrinkled structure by diethylenetriamine (DETA) and their reinforcing effects in the flexible poly (2-ethylhexyl acrylate) (P2EHA) films. Compos Part A-Appl S 84:64–75

Suggs K, Reuven D, Wang XQ (2011) Electronic properties of cycloaddition-functionalized graphene. J Phys Chem 115:3313–3317
Terrones M, Mendez ARB, Delgado JC et al (2010) Graphene and graphite nanoribbons: morphology, properties, synthesis, defects and applications. Nano Today 5:351–372
Toda K, Furue R, Hayami S (2015) Recent progress in applications of graphene oxide for gas sensing: a review. Anal Chim Acta 878:43–53
Wallace PR (1947) The band theory of graphite. Phys Rev 71:622–634
Wan X, Long G, Huang L et al (2011) Graphene - A promising material for organic photovoltaic cells. Adv Mat 23:5342–5358
Wang H, Maiyalagan T, Wang X (2012a) Review on recent progress in nitrogen-doped graphene: synthesis, characterization, and its potential applications. ACS Catal 25:781–794
Wang X, Dong X, Wen Y et al (2012b) A graphene–cobalt oxide based needle electrode for non-enzymatic glucose detection in microdroplets. Chem Commun 48:6490–6492
Wang L, Liu W, Zhang Y et al (2015a) Graphene-based transparent conductive electrodes for GaN-based light emitting diodes: challenges and countermeasures. Nano Energy 12:419–436
Wang Y, Xie Y, Sun H et al (2015b) 2D/2D nano-hybrids of γ-MnO_2 on reduced graphene oxide for catalytic ozonation and coupling peroxymonosulfate activation. J Hazard Mater (in press)
Wu ZS, Yang S, Sun Y et al (2012) 3D nitrogen-doped graphene aerogel-supported Fe_3O_4 nanoparticles as efficient electrocatalysts for the oxygen reduction reaction. J Am Chem Soc 134:9082–9085
Xia F, Farmer DB, Lin Y et al (2010) Graphene field-effect transistors with high on/off current ratio and large transport band gap at room temperature. Nano Lett 10:715–718
Xue B, Zhu J, Liu N et al (2015) Facile functionalization of graphene oxide with ethylenediamine as a solid base catalyst for Knoevenagel condensation reaction. Catal Commun 64:105–109
Yadav SK, Cho JW (2013) Functionalized graphene nanoplatelets for enhanced mechanical and thermal properties of polyurethane nanocomposites. App Surf Sci 266:360–367
Yang M, Yao J, Duan Y (2013) Graphene and its derivatives for cell biotechnology. Analyst 138:72–86
Yang Y, Gao F, Cai X et al (2015) β-Cyclodextrin functionalized graphene as a highly conductive and multi-site platform for DNA immobilization and ultrasensitive sensing detection. Biosens Bioelect 74:447–453
Yu D, Park K, Durstock M et al (2011) Fullerene-grafted graphene for efficient bulk heterojunction polymer photovoltaic devices. J Phys Chem Lett 26:1113–1118
Yu Z, McInnis M, Calderon J et al (2014) Functionalized graphene aerogel composites for high-performance asymmetric supercapacitors. Nano Energy 11:611–620
Yu P, Lowe SE, Simon GP et al (2015) Electrochemical exfoliation of graphite and production of functional graphene. Curr Opin Colloid Interface Sci (in press)
Yuan B, Shi Y, Mu X et al (2016) A facile method to prepare reduced graphene oxide with a large pore volume. Mat Lett 162:154–156
Zarotti F, Gupta B, Iacopi F et al (2016) Time evolution of graphene growth on SiC as a function of annealing temperature. Carbon 98:307–312
Zhang N, Zhang Y, Xu YJ (2012a) Recent progress on graphene-based photocatalysts: current status and future perspectives. Nanoscale 4:5792–5813
Zhang Y, Zhang L, Zhou C (2013) Review of chemical vapor deposition of graphene and related applications. Acc Chem Res 46:2329–2339
Zhang R, Li H, Zhang ZD et al (2015a) Graphene synthesis on SiC: reduced graphitization temperature by C-cluster and Ar-ion implantation. Nucl Instrum Methods Phys Res Sect B 356–357:99–102
Zhang L, Li Y, Wang H et al (2015b) Strong and ductile poly(lactic acid) nanocomposite films reinforced with alkylated graphene nanosheets. Chem Eng J 264:538–546
Zhang Y, Ma HL, Zhang Q et al (2012b) Facile synthesis of well-dispersed graphene by γ-ray induced reduction of graphene oxide. J Mater Chem 22:13064–13069

Chapter 2
Functionalization of Carbon Nanotube and Applications

Abstract Carbon nanotubes (CNTs) have unique structures, comprising diameters of few nanometers and length of several hundred nanometers, which provides outstanding mechanical, electrical, and thermal properties. Since their discovery in 1991, CNTs have received much attention and are a worldwide research subject due to their wide range of applications as biosensors, drug delivery, electrochemistry, nanoelectronics, superconductors, nanowires, graphene nanoribbons, nanocomposite materials, and so on. The functionalization treatments can enhance the usual CNT poor dispersion in solvents and improve their interactions with other materials, improving their technological application. Then, carbon nanotube is an extremely hot topic, and every day new research papers are published on this subject. This book contains complete and current reviews on CNT topics, such as synthesis, characterization, and application of functionalized CNTs. The characterization of functionalized CNTs is extremely important for determining the real physicochemical properties of the material obtained after functionalization treatments. However, this characterization is rarely addressed in books or review articles. Generally, the functionalization reviews are too wide-ranging, discussing the functionalization of various materials (e.g., nanomaterials), or too specific, analyzing only one functionalization agent (with some specific chemical group, e.g.). This book, however, proposes to discuss the functionalization of one of the most widely used nanomaterials in recent years: carbon nanotube. Thus, the reader will find information on CNT functionalization, using several functionalization agents, in the same book.

Keywords Carbon nanotubes · Synthesis · Characterization · Application · Functionalization

F.V. Ferreira et al., *Functionalizing Graphene and Carbon Nanotubes*,
SpringerBriefs in Applied Sciences and Technology,
DOI 10.1007/978-3-319-35110-0_2

2.1 Carbon Nanotube

2.1.1 Introduction

The study of nanoscience has provided the means for understanding and controlling the phenomena and manipulation of materials at the macromolecular, molecular, and atomic scales. This study enables to prepare nanomaterials, expanding the range of material applications and improving its properties. Studies on nanomaterials have expanded the scientific field with several research lines, such as mechanical, sensing, and aerospace systems (Gooding 2005; Coleman et al. 2006; Gohardani et al. 2014).

Nowadays, carbon-based nanostructures are important for several industrial applications. However, the unique carbon structures known until the 1980s were graphite and diamond. The discovery of C_{60} and other carbon fullerenes changed the status quo at that time (Kroto et al. 1985). This remarkable discovery, from that moment forward, has boosted the research in the nanoscience field. The synthesis of fullerene stimulated interests in studying other structures. Then, carbon nanotubes (CNTs) were discovered in the following decade (Iijima 1991).

CNTs, according to the concept, are graphene sheets wrapped around itself to form cylindrical tubes. These tubes consist of layers of sp^2-bonded carbon atoms where each carbon atom is connected to three others on the x–y plane. There are three basic types of CNTs, which are normally categorized: single-walled carbon nanotube (SWCNT), double-walled carbon nanotube (DWCNT), which has two

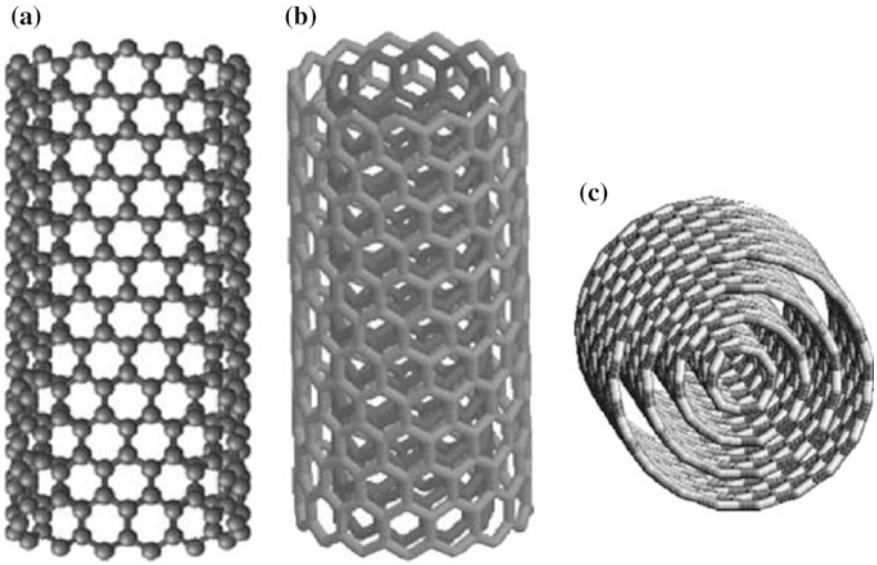

Fig. 2.1 The three types of carbon nanotubes: SWCNT (**a**), DWCNT (**b**), and MWCNT (**c**). Adapted from Loos and Schulte (2015)

Table 2.1 Typical properties of CNTs (Reproduced with the permission from Sahoo et al. 2010)

Property	SWCNT	DWCNT	MWCNT
Tensile strengh (GPa)	50–500	23–63	10–60
Elastic modulus (TPa)	~1	–	0.3–1
Elongation at break (%)	5.8	28	–
Electrical conductivity (S/m)	1.3–1.5	1.5	1.8–2.0
Thermal stability		~106	
Typical diameter	1 nm	>700 C (in air)	
Specific surface area		10–20 m^2/g	

cylindrical tubes, and multi-walled carbon nanotube (MWCNT), which has several concentric tubes (Fig. 2.1) (Sahoo et al. 2010).

CNTs have received much attention and are a worldwide research subject since their discovery in 1991 due to their wide range of applications as biosensors (Yang et al. 2010), drug delivery (Wong et al. 2013), electrochemistry (Tsierkezos et al. 2015), nanoelectronics (De Volder et al. 2013), superconductors (Pillet et al. 2010), nanowires (Zhang et al. 2015), graphene nanoribbons (Kabbani et al. 2015), nanocomposite materials (Cividanes et al. 2013), and so on.

The unique CNT structure, comprising diameters of few nanometers and length of several hundred nanometers, provides outstanding mechanical, electrical, and thermal properties, which ensures such extensive applications (Abdalla et al. 2008). The typical properties of CNTs are displayed in Table 2.1. CNT Young's moduli might range from 270 GPa to 2 TPa. However, the accurate magnitude of the CNT properties depends on the type (SWCNT, DWCNT, or MWCNT), the diameter, length, and the chirality of the material. The CNT chirality is determined by the CNT fabrication process (Abdalla et al. 2008).

2.1.2 Synthesis

Iijima started laboratory scale production of CNT in 1991 using the arc-discharge method. Since then, CNTs have been among the most researched materials in the recent times. Many other production methods were developed over the last two decades in order to obtain cheaper methods and large-scale production. Figure 2.2 summarizes the current production methods.

2.1.2.1 Chemical Vapor Deposition (CVD)

Chemical vapor deposition is the most widely accepted method for CNT fabrication, and this is due to its simplicity, low-temperature operation, bulk, and low-cost production (Song et al. 2009). CVD was developed in the 1960s and was successfully used in the carbon fiber production (De Greef et al. 2015). In 1996, CVD

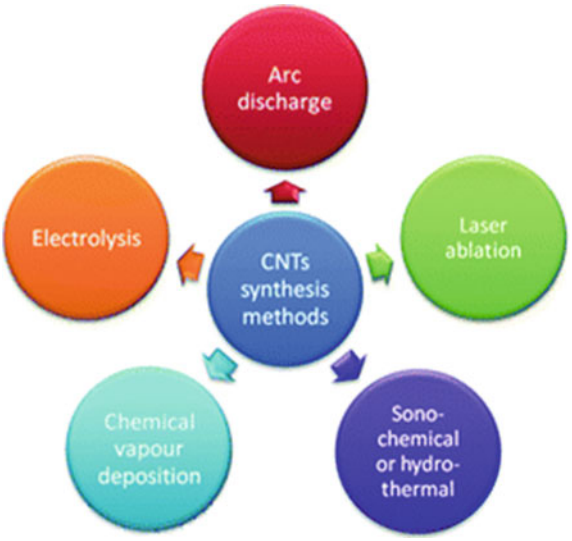

Fig. 2.2 Current methods of CNT synthesis. Adapted from Prasek et al. (2011)

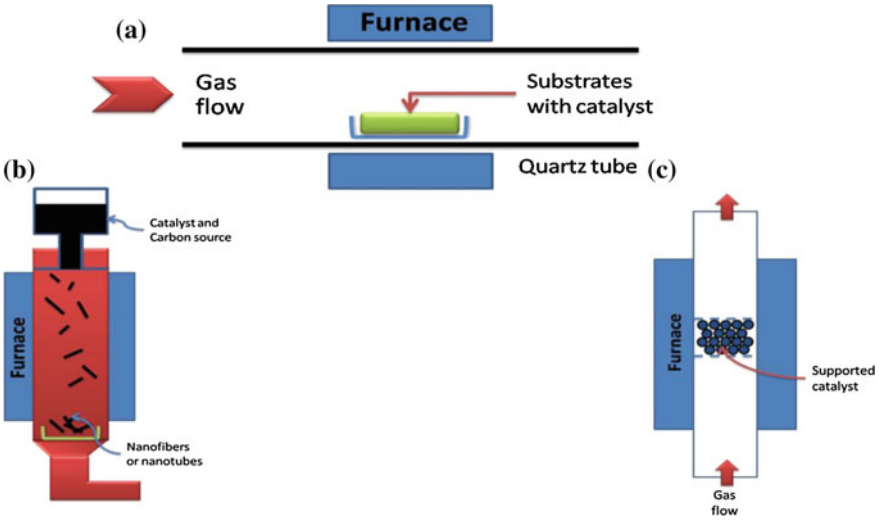

Fig. 2.3 Diagram scheme of a CVD setup. **a** Horizontal furnace, **b** Vertical furnace and **c** Fluidized bed reactor (Szabó et al. 2010)

emerged as a potential method for large-scale production and synthesis of CNTs (Li et al. 1996).

The CNT synthesis involves a flow of hydrocarbon gases or volatile carbon compounds through a tubular reactor in an inert gas environment, to prevent the

burning of CNTs. Ferrocene is normally the catalyst, which acts as nucleation sites and triggers the growth process. The total procedure lasts about 15–60 min (Kumar and Ando 2010; Antunes et al. 2011). Temperatures higher than 600–1000 °C are required for obtaining SWCNTs. Otherwise, MWCNTs are formed at lower temperatures, between 300 and 800 °C (Li et al. 2004) as shown in Fig. 2.3.

2.1.2.2 Arc Discharge

Arc discharge was the method used by Iijima in the early 1990s for synthesizing CNTs. The process takes place in a helium atmosphere of 100 Torr with two graphite electrodes at about 1 mm of distance between them (Fig. 2.4). CNTs grow on the tip of the negative electrode, and the arc occurs under a current of 200 A at 25 V (Iijima 1991; 1993).

Several improvements in the synthesis method were tested in order to improve the synthesis, obtaining different kinds of CNTs, such as increasing the helium pressure to improve the reaction yield or by changing the helium to N_2, CF_4, or some organic gases (Shimotani et al. 2001).

CNTs can be produced by replacing the graphite electrodes with metals, such as Ni, Fe, Co, Gd, and Y (Liu et al. 2014). The electrical current of the arc is another important variable of the process, where low currents improve the MWCNT quality and high currents favor the SWCNT production (Ando et al. 2000).

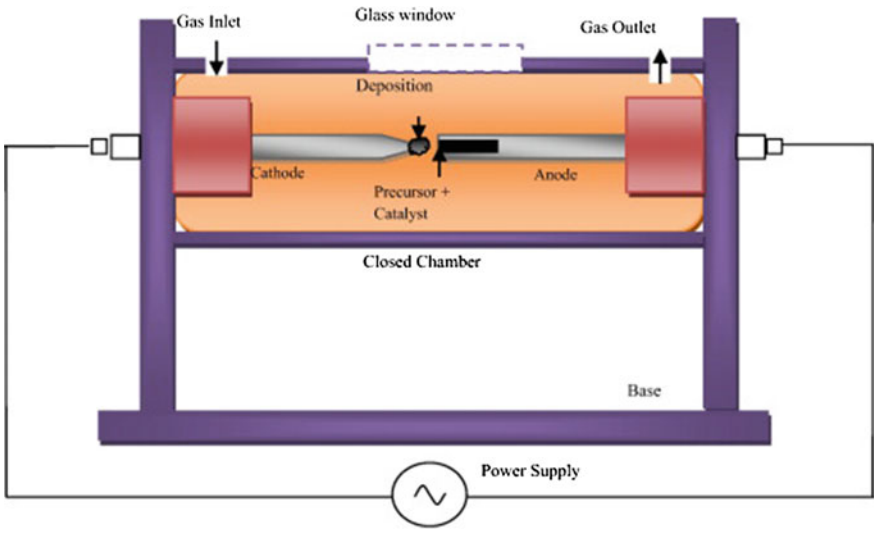

Fig. 2.4 Diagram of an arc plasma discharge setup (Arora and Sharma 2014)

2.1.2.3 Laser Ablation

The first CNT synthesis using this method was reported in 1995, with much better control over the growth of CNTs than the arc-discharge method (Guo et al. 1995). In this method, the same conditions for arc discharge are used to operate laser ablation (Fig. 2.5). This synthesis uses graphite as the carbon source, doped with small quantity of metallic catalyst (Co, Ni, and Pt) on a quartz tube, at very high temperatures (between 800 and 1500 °C). Graphite is vaporized with a laser beam pulse at an inert gas atmosphere, at pressure of 500 Torr (Liu et al. 2014; Mittal et al. 2015). Double-pulsed laser increases the production yield of CNTs, always resulting in single-walled CNTs (Thess et al. 1996; Goddard et al. 2012).

The laser ablation technique is the costliest method to produce CNTs as it requires high power. Furthermore, there are some impurities in CNTs produced by this method, such as metal catalysts and amorphous carbon. On the other hand, SWCNT can be synthesized without the presence of MWCNT, unlike the arc-discharge method, which can result in a mixture of single-walled and multi-walled CNTs. So, this technique could be useful for some applications which would only need SWCNT (Mittal et al. 2015).

2.1.2.4 Electrolysis

Initially, this method was used to generate fullerene, but in 1996, CNTs were grown electrochemically for the first time. The procedure requires a current of 3–20 A, up to 20 V between graphite electrodes immersed in molten LiCl, under 100–150 Torr, in an argon atmosphere at 600 °C for 2 min (Fig. 2.6) (Hsu et al. 1996; Szabó et al. 2010).

However, until 2002, this method had been used only to produce MWCNTs, when SWCNTs were successfully produced. The optimum conditions to produce SWCNT require a temperature of 810 °C, current of ∼4.5 A, and voltage between 9 and 12 V (Bai et al. 2002).

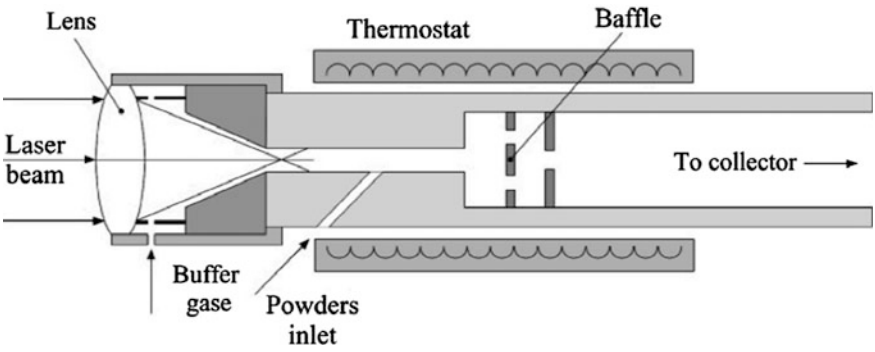

Fig. 2.5 Diagram scheme of a laser ablation setup (Bolshakov et al. 2002)

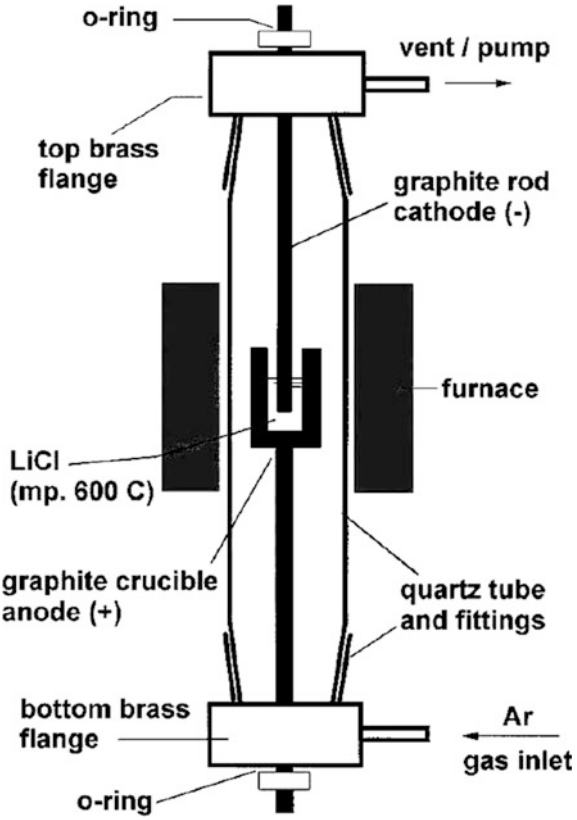

Fig. 2.6 Diagram scheme of an electrolysis method setup (Hsu et al. 1996)

The electrolysis method is not largely used due to the low purity of the obtained CNTs. On the other hand, however, there are some possibilities to control the CNT structures and morphologies optimizing the electrolysis conditions, such as using LiCl, KCl, NaCl, and LiBr (Terrones 2003; Szabó et al. 2010).

2.1.2.5 Hydrothermal

The hydrothermal method uses a heterogeneous reaction in the presence of aqueous solvents or metallic material, taking place in a closed system, under pressure and temperature conditions to dissolve and recrystallize insoluble materials (Byrappa and Adschiri 2007; Szabó et al. 2010). For example, CNTs were prepared using an ethylene glycol ($C_2H_4O_2$) solution and metallic Li as starter material, under 60–100 MPa and at 730–800 °C (Gogotsi et al. 2002).

An important aspect for the synthesis of CNTs using the hydrothermal method is the CNT production with no catalyst metal at 800 °C, resulting in MWCNT with diameter of $\sim$10 nm and length of hundreds of nanometers (Moreno et al. 2000;

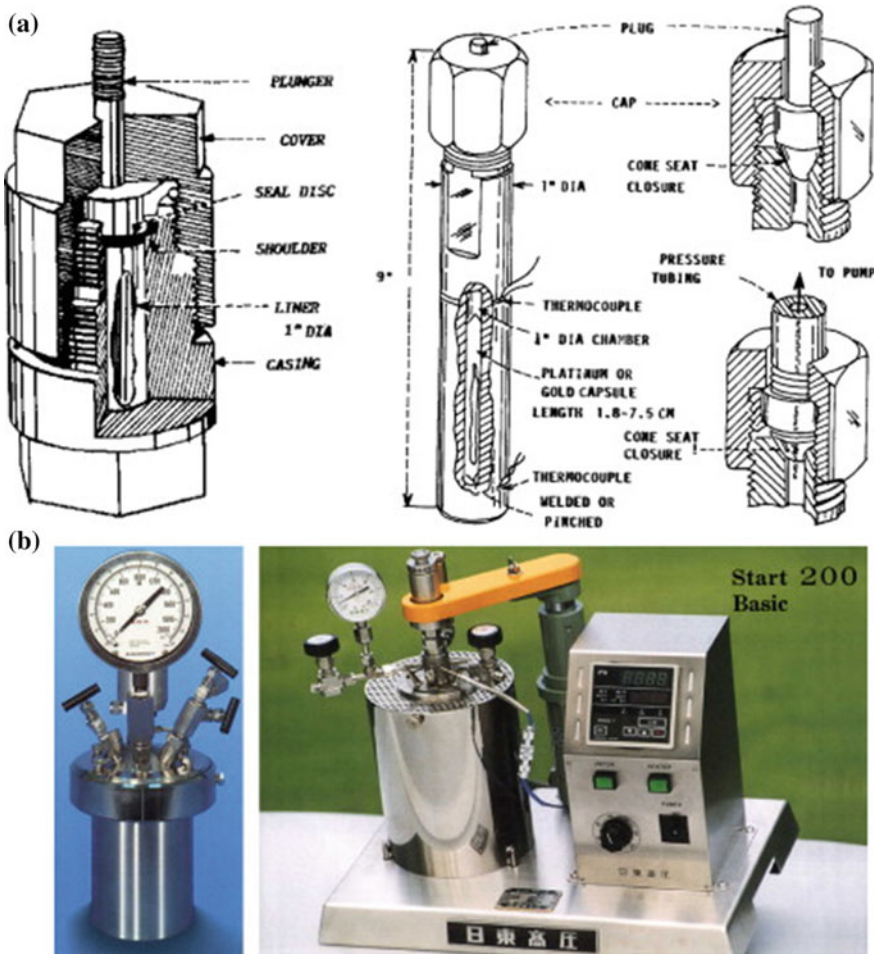

Fig. 2.7 Diagram scheme of **a** a common hydrothermal reactor and **b** a commercial autoclave used in the hydrothermal processing (Byrappa and Adschiri 2007)

Gogotsi and Presser 2013). Figure 2.7 shows a usual autoclave design and a commercial model.

Temperature and pressure are parameters that greatly affect dissolution, which are very important in the hydrothermal process. So far, there is no report of SWCNT preparation or commercial production of CNTs using this technique (Ren et al. 2012). In this procedure, the highlight is the environmentally friendly technology due to the absence of hazardous elements in the reaction, in addition to the moderate pressure and temperature, the low energy consumption, and the high yield (Gogotsi and Libera 2000).

Table 2.2 CNT synthesis methods' advantages/disadvantages

Method	Product	Advantage	Disadvantage
CVD	SWCNT ϕ 0.6–4 nm MWCNT ϕ 10–240 nm Medium to high purity	Scaleable up to industrial production, diameter controllable	SWCNT and MWCNT mixture
Arc discharge	SWCNT ϕ 0.6–1.4 nm MWCNT ϕ 1–3 nm Medium purity	Few defects, no catalyst, not too expensive, open air	Carbon impurities, other nanoparticles, short CNTs
Laser ablation	SWCNT ϕ 1–2 nm MWCNT ϕ 1–3 nm Low purity	Good quality, highest yield, narrower distribution of SWCNT diameter	Very high-cost, impure CNTs
Electrolysis	MWCNT ϕ 10–20 nm SWCNT ϕ 1.3–1.6 nm Low purity	Cheap reagents, simple apparatus, low energy consumption	Difficult control, poor purity
Hydrothermal	MWCNT ϕ 5–8 nm Low purity	Easy process, low temperature	Low-scale production, many defects, difficult controls
Ref.	Szabó et al. (2010), Shah and Tali (2016)	Guo et al. (1995), Szabó et al. (2010)	Liu et al. (2014), Szabó et al. (2010)

The CVD method seems to be the best one for large-scale production of MWCNTs among all the methods shown in this report. However, the production yield of SWCNTs has not yet achieved an industrial scale. New techniques for CNT production and improvements and adaptations of the regular methods are always emerging. However, the CNT production with elevated purity, constant size, large scale, and low cost remains as the biggest concern in the academic community (Loos and Schulte 2015). Table 2.2 summarizes some aspects of the methods discussed in this chapter.

2.1.3 Carbon Nanotube Functionalization

CNT production is performed by several methods, and each one can result in different CNT structures (Wang and Arash 2014; Rahmat and Hubert 2011). Therefore, each method can result in CNTs with different mechanical, thermal, and electrical properties (Jorio et al. 2008; Lee 2015). Basically, the magnitude of these properties is highly dependent on its synthesis method, purification treatment, and further surface treatments (Sahoo et al. 2010; Cividanes et al. 2015).

CNTs are very likely to aggregate and form bundles, limiting their superior properties and causing poor solubility in both aqueous medium and non-aqueous medium. The CNT insolubility is due to its high van der Waals attractions between the tubes (Li et al. 2008; Alpatova et al. 2010; Khan et al. 2010). Over the past decade, a variety of strategies were devised to improve their solubility, dispersibility, and surface interaction (Khan et al. 2010). Chemical functionalization can enhance the usual poor dispersion in solvents, (Ferreira et al. 2015), improve their interactions with other materials (Francisco et al. 2015), and change the cure behavior of some polymers (Abdalla et al. 2008), improving their technological application. Often, the CNT bundles are broken up by ultrasonication, followed by the attachment of a chemical agent, which "wraps up" the CNTs. This attachment changes the CNT surface, preventing their reaggregation (Husanu et al. 2008).

Commonly, the functionalization of CNTs is labeled as non-covalent and covalent. The non-covalent modification is related to the intermolecular interaction between CNT walls and a chemical group by van der Waals forces. However, the covalent functionalization is based on the formation of a covalent chemical bonding between CNT wall and the functionalization agent (Loos and Schulte 2015).

2.1.3.1 Covalent Functionalization

Functionalization is based on a covalent linkage of functional groups on the outer CNT wall. These functional groups can react with carboxylic groups (–COOH) of CNTs and other oxygenated group formed during an oxidative reaction process. Carboxylic groups located on CNT defects attach to several chemical groups (Meng et al. 2009). The covalent functionalization occurs by a change on the carbon hybridization (sp^2 to sp^3) with simultaneous loss of the local conjugation. This functionalization type requires very reactive reagents, usually with high yield of functionalization (Balasubramanian and Burghard 2005).

CNTs are functionalized with different chemical groups, such as carboxylic groups (–COOH) (Francisco et al. 2015), alkyl ($–C_6H_{11}$) (Ferreira et al. 2015), amide group (Cividanes et al. 2014a), and phenyl group (Mohamed et al. 2015) (Balasubramanian and Burghard 2005). Figure 2.8 shows the change in the structure caused by the functionalization.

The number of papers on CNT covalent functionalization has increased substantially since the discovery of CNT (Terrones 2003; Mittal 2011). Ajayan et al. (Ajayan et al. 1994; Moniruzzaman and Winey 2006) were the first to publish the CNT use—as filler in polymer nanocomposites, since then this subject has increased in importance and in number of works. This extensive investigation was performed with several covalent modifications, each one providing a different purpose. Imidazole functionalization was conducted to improve the electrical conductivity and enhance the interfacial adhesion. CNTs treated with cloridic acid were reacted with 3-aminopropylimidazole, attaching the imidazole groups (IL) on the CNT surface. When embedded in a polymer matrix, CNTs-IL demonstrated an

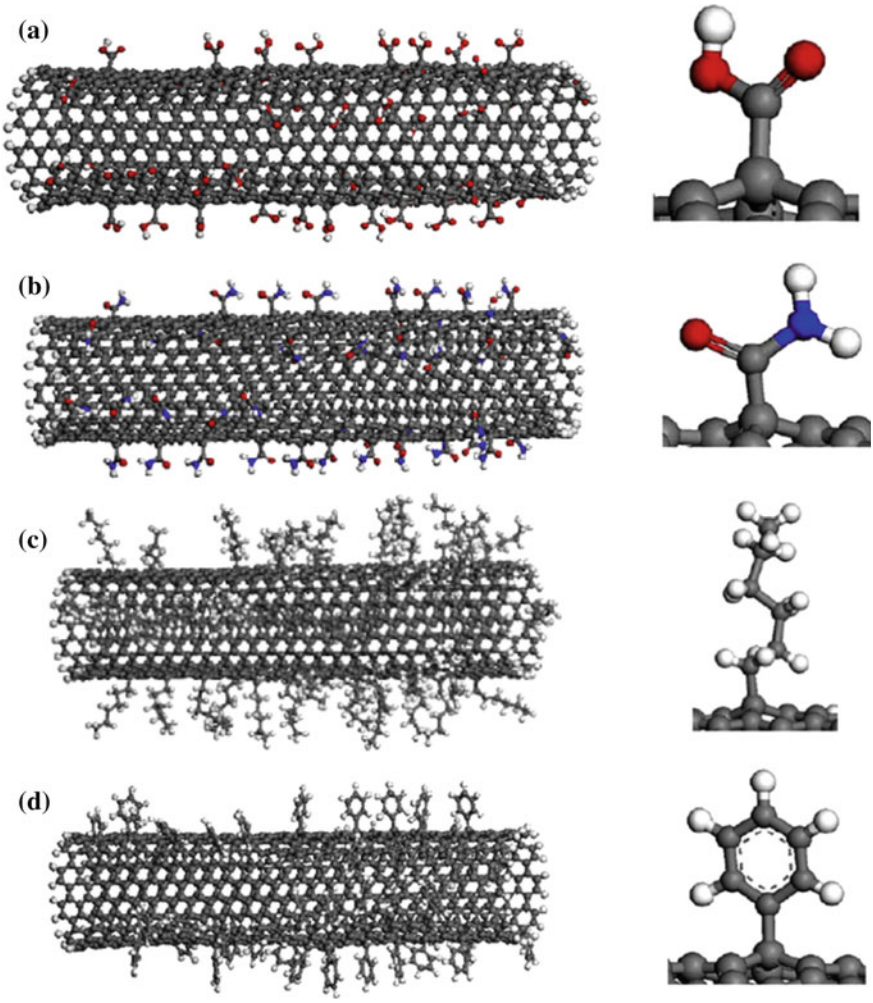

Fig. 2.8 CNTs functionalized with different chemical groups. **a** carboxylic groups (–COOH); **b** amide groups ($–CONH_2$); **c** alkyl groups ($–C_6H_{11}$); **d** phenyl groups ($–C_6H_5$) (Loos and Schulte 2015)

enhanced DC conductivity. A high-conductivity and lightweight multi-functional composite was created for potential aerospace applications (Wang et al. 2012).

Another experimental research group reacted SWCNTs with glycidyl methacrylate (GMA), which was able to graft epoxide onto single-walled CNTs. An epoxy polymer nanocomposite was made with the CNTs-GMA and demonstrated high degree of exfoliation and homogeneous dispersion in the polymer matrix. The overall mechanical properties of epoxy resin-based nanocomposites were extensively improved (Wang et al. 2008).

Medical applications of the functionalized CNTs have been examined. SWCNTs have been functionalized by proteins, collagen, lipids, and single-stranded DNA, others. By attaching ligands to their surface, as antibodies, peptides, folic acid, etc., some CNT properties can be improved, such as targeting and selectivity.

Functionalization of CNTs has been investigated by theoretical and simulation methods. Mechanical properties and buckling behavior of CNTs functionalized with diethyltoluenediamines (DETDA) were analyzed. The results of this research showed critical buckling force, and an increase in the Young's modulus was almost linear, showing the effectiveness of polymer grafted with CNTs for nanocomposite application (Ansari et al. 2015).

Kuan and Huang filled a polymer with MWCNT, where methyl groups ($–CH_3$) were the functional group. The results showed an increase in the thermal resistance at the interface. Simulation and empirical tests showed that the CNT surface modification had an adverse effect on the thermal transport of the nanocomposite (Kuang and Huang 2015).

There are several approaches for CNT functionalization using the unique properties of CNTs. The critical challenge is to find the best methods to improve a specific property, whether mechanical, electrical, optical, etc. Despite the functionalization with various chemical groups, such as carboxylic, amide, alkyl, phenyl, e-caprolactone, L-lactide, styrene, and imide, there are still challenges and opportunities to be overcome in order to improve the CNT properties. One of the main challenges is to achieve the optimal functionalization of CNTs for a particular application (Park et al. 2003; Baskaran et al. 2004; Zeng et al. 2006; Chen et al. 2007).

2.1.3.2 Non-covalent Functionalization

The covalent and non-covalent functionalizations make CNTs soluble in aqueous or organic solutions, especially in volatile organic solvents or strong acids (Huang et al. 2007).

In recent years, non-covalent surface modifications of CNTs using amphiphilic molecules have been used as an alternative strategy to functionalize CNTs. Low molecular weight surfactant, amphiphilic polymer, or some organic molecules are used as non-covalent functionalization agents (Sa et al. 2008; Alpatova et al. 2010). The chemical and mechanical properties of CNT are only weakly disturbed by a non-covalent functionalization when compared to covalent surface functionalization as no chemical bond is formed between the adsorbed molecule and CNT.

Non-covalent functionalization usually introduces fewer defects in the graphitic structure, which is preferable for solubilization enhancement. This enhancement is due to the π–π stacking or hydrophobic interactions formed between the adsorbed molecules and CNT surface. This kind of interaction maintains the maximum intrinsic characteristics of an individual nanotube, without altering its original structure and electronic properties (Lee et al. 2007; Li et al. 2008; Ghosh et al. 2010). Multi-walled CNTs (MWCNTs) are preferable for a functionalization

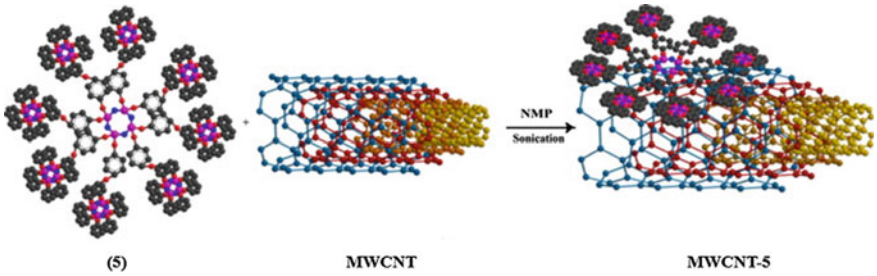

Fig. 2.9 Molecule attachment on CNT surface via non-covalent interaction (Okutan et al. 2014)

process than the SWCNT or DWCN, because they are less likely to damage during the process (Kasperski et al. 2014).

Dispersion, via non-covalent functionalization (Fig. 2.9), is based on the direct contact between CNT and the dispersant molecule. This CNT modification facilitates the disaggregation/debundling of CNT bundles into smaller agglomerates or even individualization. The disaggregation is due to the CNT solution stabilization enhanced by the steric impediment or electrostatic repulsion, among functional groups or both. The suspension stability of CNT functionalized non-covalently is a function of the type and concentration of the dispersant, the CNT length, and the presence of inorganic salts in solution (Alpatova et al. 2010; Ghosh et al. 2010; Khan et al. 2010).

The CNT functionalization with porphyrin molecules provides CNTs with some intrinsic properties of porphyrins, such as luminescence, photovoltaic effects, and biocompatibility. *Meso*-(tetrakis-4-sulfonatophenyl) porphine (TPPS4) and 5,15-bis (3,5-di–tert-butylphenyl) porphyrin were used in a non-covalent functionalization of CNTs, and they made CNTs soluble in aqueous media (Huang et al. 2007).

Several surfactants and oligomeric or amphiphilic polymers were used to disperse CNT in aqueous media, considered to be quite attractive and with many potential applications (Alpatova et al. 2010; Chen et al. 2013). The tail of a hydrophobic surfactant can adsorb at a hydrophobic surface of CNT, providing multiple van der Waals interactions, yielding a chemical bond strong enough to form stable complexes (Behnam et al. 2013).

The attachment of PEG chains onto a CNT surface is widely used to improve both colloidal stability and biocompatibility. Pluronic has two terminal PEG blocks and a middle poly(propylene oxide)(PPO) block and is used as a functionalization agent, yielding good dispersions. An amphiphilic molecule, with an aromatic component and a PEG chain, is a good candidate for dispersing CNTs in water with enhanced long-term stability (Lee et al. 2007). Polyethyleneimine (PEI) is a hydrophilic molecule with a polar head group, which can functionalize CNT with high water solubility (Behnam et al. 2013). The surfactants sodium dodecyl sulfate (SDS), cetyl trimethyl ammonium bromide (CTAB), and nonionic Tween-20 (TW) are used as dispersants to improve CNT dispersion in a water medium (Ponnamma et al. 2014).

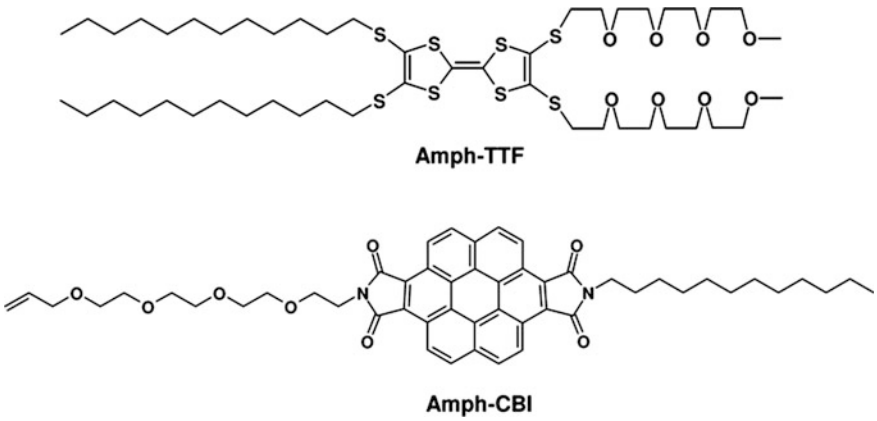

Fig. 2.10 Amph-TTF and Amph-CBI molecules used on non-covalent functionalization (Ghosh et al. 2010)

Molecules containing aromatic groups are believed to adsorb onto graphite surface more strongly than aliphatic molecules, due to the π–π interaction between the graphite surface and the aromatic component of amphiphilic molecules, involving van der Waals and electrostatic interaction (Alpatova et al. 2010; Sanz et al. 2011; Okutan et al. 2014). Two other molecules that can be used for non-covalent functionalization are shown in Fig. 2.10.

Tetrathiafulvalene (Amph-TTF) has two dodecyl chains at one end and also has tetraethylene glycol chains. In addition, coronene bisimide (Amph-CBI) has a dodecyl and a tetraethylene glycol chain (Fig. 2.10). These molecules have large planar aromatic surfaces, which can strongly attach to the side walls of SWCNTs through π–π stacking interactions. The long alkyl chains promote the solubility of CNTs in organic solvents (Ghosh et al. 2010).

Tetrazine molecules can adsorb on MWCNT surfaces by a non-covalent functionalization, generating a π–π stacking with the graphitic sidewalls of MWCNTs. Their amino groups (NH_2) are useful not only for dispersing MWCNTs in epoxy matrices but also to improve the interface properties between MWCNTs and epoxy. Amino group of tetrazine molecules can modify the electrical properties of MWCNTs due to electron donation effect of the nitrogen atoms attached on the MWCNTs (Zhang et al. 2012b).

The stacking of the polycyclic aromatic hydrocarbons (PAHs) on CNTs is a viable approach to functionalize CNTs by a non-covalent bonding, which can prevent a decrease in electrical properties. Non-covalent functionalization using amphiphilic polymer containing pyrene pendants can form π–π stacking interactions with the aromatic surfaces of CNTs (Ryu and Han 2014; Zhang et al. 2012a). The amphiphilic copolymers of PVP-co-PAH (polyvinylpyrrolidone copolymer polyciclic aromatic hydrocarbons) with pyrene pendants were synthesized by Zhang et al. (Zhang et al. 2012a). They were used as functionalization agents, and

the PVP groups modified the CNT surfaces, achieving good dispersion in water and organic solvents, such as 1-aminopyrene and 1-nitropyrene (Jin et al. 2013; Madec et al. 2013). 1-(hydroxymethyl) pyrene was adsorbed on CNTs by π–π stacking interaction, improving the CNT solubility and reactivity (De Filpo et al. 2015). Pyrene-appended spiropyrans was non-covalently attached to CNT, and a light switching property was observed (Perry et al. 2015).

Other non-covalent functionalizations of CNTs, such 2-aminoethanol surfactant ($H_2NCH_2CH_2OH$) in the presence of sodium hydroxide, are an efficient way to functionalize CNTs for developing the electrical conduction property of MWCNT/epoxy nanocomposites (Li et al. 2008).

Sulfonation of CNTs is an efficient way to increase the dispersion of CNTs due to the high hydrophilicity of $–SO_3H$ group. The functionalized CNTs showed high dispersibility in deionized water and good electrical conductivity due to the fact it maintained the intrinsic sp^2 structure of MWCNTs (Fu et al. 2011).

2.1.3.3 Other Methods of Carbon Nanotube Functionalization

The search for functionalization optimization led to the development of other methods to fill the gaps left by covalent and non-covalent functionalization, such as click chemistry functionalization, one of the most successful methods used in the preparation of CNTs for biosensing applications. The 1,3-dipolar cycloaddition (CuAAc) reaction catalyzed by Cu (I) between arylazido-decorated N_3-SWCNTs and alkyne-terminated organic/organometallic compound can also immobilize biological sensing elements on CNTs and change the optical and electronic properties of CNTs for the aforementioned application (Boujtita 2014). There has been an increase of papers related to click chemistry functionalization of CNTs. Sahoo reported (Sahoo et al. 2010) the attachment of several different functionalization agents on CNTs via click coupling, such as gold–nanoparticles–N_3.

Defect functionalizations are a functionalization method obtained by an oxidation process. Oxygen functionalities (carboxyl, phenolic hydroxyl, ketonic carbonyl, lactone, etc.) modify CNT from a hydrophobic to a hydrophilic material, improving the dispersion in solvents and the chemical reactivity. The oxidation process in a liquid phase is frequently employed for this functionalization method by immersing CNTs in many strong oxidant reagents such as $KMnO_4$, H_2SO_4, HNO_3, and H_2O_2. On the other hand, gas-phase oxidation is a more convenient and cleaner method. Among oxidant gases, ozone has several advantages such as low cost, easy accessibility from ozone generator, and sustainability. Furthermore, the superior reactivity of ozone allows functionalizations to be conducted at room temperature (Zhang and Xu 2015; Xia et al. 2016).

The introduction of oxygen groups on the surface of CNTs by covalent functionalization causes damage in the ordered structure of CNTs, which is a disadvantage to some application, for example, adsorption, electrode for electric double-layer capacitor (EDLC), catalyst support, energy storage, and fuel cells. Electrochemical techniques can control the accuracy of the functionalization

process without much change on the wall structure of CNTs (González-Gaitán et al. 2015). This method can take place with small amount of reagents and samples, at room temperature and in atmospheric pressure. Additionally, the reaction conditions are easily reproducible, and it is simple to interrupt the reaction, providing an accurate reaction control (González-Gaitán et al. 2016; Polo-Luque et al. 2013).

The wide variety of methods, such as covalent, non-covalent, click chemistry, electrochemical, and defect functionalizations, increases the importance of CNTs in the technological applications and opens a new field for nanomaterials based on the use of CNTs.

2.1.4 Carbon Nanotube Applications

CNTs have been the focus of several researches due to their exceptional mechanical, electronic, and structural properties that make them very attractive materials (Lawal 2016). The excellent mechanical and electrical properties of CNTs, along with other multi-functional characteristics, provide an entire new class of composite materials with high potential in structural and functional applications (Paradise and Goswami 2007; Thostenson et al. 2001).

Recently, there has been considerable research interest in functionalized CNTs and their applications. Potential practical applications have been reported in several areas of science, medicine, and engineering. CNTs and CNT-based materials have presented major development in the reinforcement of high-performance composites, electronic and optoelectronic devices, chemical sensors, optical biosensors, energy storage, field emission materials, catalyst support, nanoprobes for meteorology, and biomedical and chemical investigations. These are just some of the possibilities explored, but new applications will also be developed with new studies conducted in the years to come (Paradise and Goswami 2007; Lawal 2016).

2.1.4.1 CNT/Polymer Matrix Composites

Polymers have a wide range of applications, which include advanced engineering such as car and airplane parts, optical components, electronic packaging, insulating, semiconducting materials, tubing, and liquid crystal display, among others. Despite its favorable characteristics (lightweight, easy molding, and low price), polymers have some limitations, such as low melting temperature, low strength, and time-dependent liquid-like flow. The discovery of CNTs by Iijima (1991) opened the door for improving the mechanical, electrical, and other important properties of polymers, emerging as a new class of functional material for structural and biomedical applications, energy storage, and sensors (Montazeri and Naghdabadi 2009).

The first work to study the addition of CNTs as reinforcement in the polymer matrix was performed by Shaffer and Windle in 1999. They studied the thermomechanical and electrical properties of nanocomposites with poly(vinyl alcohol)

and CNTs. They observed that the stiffness of the nanocomposites at room temperatures was relatively low, but was considerably high at elevated temperatures. In addition, these nanocomposites showed the same percolation behavior observed in other fiber-filled systems. They concluded that nanotubes could be used as a polymer modifier, particularly to be used at high temperatures (Shaffer and Windle 1999).

2.1.4.2 Mechanical Applications

In the field of mechanics, it is known that CNTs exhibit excellent mechanical properties, with Young's modulus as high as 1.2 TPa and tensile strength of 50–200 GPa. These exceptional characteristics combined with low density, high surface area, and high aspect ratio make CNTs strong candidates as nanocomposite reinforcing materials. However, the successful addition of CNTs in polymers depends strongly on the dispersion state of the nanofillers. A good dispersion prevents the aggregation of CNTs, avoiding stress concentration and increasing the CNT surface area available for bonding with the polymer matrix. SWCNTs and MWCNTs are used as reinforcement in the polymer nanocomposite production, using both thermosetting and thermoplastic polymers as matrices. The most widely used polymer matrices are as follows: epoxy, polyurethane, phenol formaldehyde resins (thermosettings), polyethylene, polypropylene, polystyrene, and polyamide (thermoplastics) (Ma et al. 2010; Cividanes et al. 2014b).

Composites reinforced with functionalized CNTs have been studied by many authors. Cividanes et al. (2013) used micrographs of the cryogenically fractured surfaces of epoxy resin/carbon nanotube composites and concluded that non-functionalized CNTs were not well dispersed in the epoxy matrix and the adhesion between CNT and epoxy was poor. Acid functionalization improved the adhesion between CNT and resin and also promoted little improvement in the CNT dispersion. However, nanocomposites prepared with amino-treated CNTs showed the most homogeneous dispersion and a better interfacial bonding between CNT and epoxy. They also suggested that the presence of CNTs, functionalized or not, increased the cure degree of the samples.

Some studies showed an increase in mechanical properties by adding functionalized CNT in a polymer matrix. Hong et al. (2015) reported an enhancement on thermal and mechanical properties of functionalized CNT/epoxy nanocomposites. CNTs were functionalized with carboxyl groups and dispersed in a polymer containing an epoxide group. The elastic modulus and storage modulus of the functionalized CNT/polymer nanocomposites increased by 100 % and 500 %, respectively, in relation to the pure polymer. Furthermore, the thermal stability of the functionalized CNT/polymer was higher than the pristine CNT/polymer nanocomposite.

Shi et al. (2012) prepared nanocomposites with high-density polyethylene (HDPE), SWCNT, MWCNT, and hydroxylated MWCNT. They observed an increment of 40–60 % in the mechanical properties due to CNT interactions with

the matrix. They also observed that CNT had antioxidant ability, increasing the oxidation induction temperature (OIT) and the oxidation induction time (OIt). Based on their measurements, the CNT antioxidant ability was in the following order: MWCNT-OH > MWCNT > SWCNT.

Ryu and Han (Ryu and Han 2014) used a melt-compounding method to obtain nanocomposites where non-functionalized CNTs and non-covalent functionalized CNTs were used as reinforcement in polyamide (PA). CNTs were functionalized with tetrahydrofuran (THF). The nanocomposite of PA/functionalized CNTs showed a much higher flexural modulus in comparison with the nanocomposite of PA/non-functionalized CNTs. Furthermore, the nanocomposites with functionalized CNT exhibited better electrical properties and the most homogenous CNT dispersion in the PA matrix.

The reinforcement of elastomers has also been performed. Liu et al. (Liu et al. 2016) prepared samples of vulcanized silicone rubber nanocomposites reinforced with surface-modified CNTs at room temperature. Firstly, an acid functionalization was performed, and then, these CNTs were treated with polyester-modified polydimethylsiloxane (BYK-310). They observed a better dispersion of CNTs in the silicone rubber matrix after BYK-310 CNT treatment. For the nanocomposite using non-functionalized CNTs, the mechanical properties were relatively lower. The nanocomposite prepared with acid-treated CNTs showed a slightly improved mechanical property, while the nanocomposite prepared with CNT treated by BYK-310 presented an outstanding enhanced mechanical property.

2.1.4.3 Electrical Applications

The composites formed by CNTs and polymer can improve the electrical properties of some materials (Paradise and Goswami 2007). CNTs have some advantages over regular materials, such as high aspect ratio and excellent electrical conductivity. These properties facilitate the formation of conducting networks, transforming insulating polymers into conducting polymers (Ma et al. 2010). Therefore, CNTs and polymer-based nanocomposites are currently attracting much attention due to their use in flexible electronics, antistatic and electromagnetic interference shielding, and sensor applications (Cesano et al. 2013).

CNT functionalization significantly influences the electrical conductivity of the nanocomposites due to their increased CNT dispersion, leading to the formation of conducting networks. However, functionalization treatment must be performed carefully in order to not insert a large number of heterogeneous atoms into the network, which act as a barrier to electrons, reducing the electrical conductivity. Furthermore, this treatment can damage the nanotube walls causing defects and reducing the aspect ratio, which is the case of acid functionalization (Ma et al. 2010).

The development of nanocomposite materials based on conducting polymers and CNTs for sensitive and selective sensors has been the focus of attention, especially for toxic chemical detection (Badhulika et al. 2014; Kumar et al. 2012). However, a

good dispersion of CNTs is crucial for achieving better performances on the polymer matrix. The surface functionalization is capable of producing a homogeneous dispersion, performed by a stronger interaction between CNTs and polymer chains. The CNT functionalization can enhance the number of CNT sites that interact with analyte, increasing the intra- and interchain mobility of charge in the polymer chains or even changing the electron-donor or gas-acceptor properties of the nanocomposites (Verma et al. 2015).

Verma et al. (2015) produced nanocomposite films with carboxyl (–COOH)-functionalized MWCNT and poly(m-aminophenol) (PmAP) by in situ chemical oxidation polymerization. They studied the sensing properties of detection of aliphatic alcohols. The results showed that a site-selective interaction occurs between the conjugated PmAP backbone chains and the bonded surface of functionalized MWCNTs. In addition, X-ray analysis showed that the addition of a small quantity of functionalized CNTs into PmAP significantly increases the crystallinity of the PmAP and substantially improved the sensor response to aliphatic alcohol vapor when compared to pure PmAP.

Due to the intense increase in electricity demand, many studies are being developed in the area of solar cells, especially in organic solar cells. CNTs are used as a pathway for electron transport in which charges are transported quickly between the interfaces of the electrodes with minimal loss, and as a consequence, there is high power conversion (Bounioux et al. 2012).

Cakmak et al. (2015) studied nanocomposites with octadecylamine-functionalized SWCNT on a bulk heterojunction of organic solar cells. Four solar cells were produced with different concentrations of CNT (0, 0.01, 0.001, and 0.001 wt%) under similar process conditions. The addition of functionalized CNTs slightly increased the optical absorption of the active layer of the solar cells, and the open-circuit voltage presented no significant changes. However, the photovoltaic measurements (current density potential curves) showed that the cell comprised with 0.001 wt% of CNT was 31.8 % more efficient compared to the cell with no CNTs. According to the authors, this is due to the nanosized pathways of CNT in the interior of the device, which enhance the mobility of electrons.

Studies about electromagnetic interference (EMI) showed a problem related to the increase in sensitivity of electronic devices (Zhao et al. 2015). The addition of CNTs as nanofillers into composites is a new alternative for providing EMI shieldings, due to their exceptional dielectric properties. Surface functionalization of CNTs improves the compatibility of CNTs on the polymer matrices and enhances its electrical properties.

2.1.4.4 CNT/Ceramic Matrix Composites

Although most research in the development of nanocomposites is focused on nanotube-based polymer nanocomposites, great attention has been given to the development of metal and ceramic matrix composites with nanotube as reinforcement. Ceramics are known to have high stiffness and excellent thermal stability.

However, their brittleness is a barrier for expanding its use as structural materials. Due to resilience and flexibility of CNTs, their addition to ceramics can be particularly advantageous in terms of mechanical properties. This combination can produce nanocomposites with excellent toughness and creep resistance combined with high-temperature stability. Therefore, efforts have been made to develop new advanced materials with better properties by adding CNTs in the ceramic matrix (Thostenson et al. 2001; Barabás et al. 2015).

The production of nanocomposites with CNTs and ceramic matrices also has the obstacle of low dispersion, which reduces the mechanical properties of the final material. Covalent functionalization and non-covalent functionalization are one of the ways to enhance dispersion and, consequently, to achieve greater homogeneity. Zaman et al. (2012) produced nanocomposites with functionalized SWCNT in an alumina matrix. They studied the effect of different functional groups (COOH or OH) on SWCNT with some alumina properties, such as grain size, hardness, fracture mode, and density. The addition of CNT to alumina changed the fracture mode from intergranular and transgranular combination to basically intergranular, since CNTs are located mainly between the grains. The relative density of the nanocomposite dropped from 99.95 to 97.78 % when compared to pure alumina. They attributed this behavior to the small degree of CNT agglomeration. There was a decrease in grain size while the hardness was basically the same for both.

Many ceramic materials, such as hydroxyapatite (HAP), have been the focus of attention due to their applications as implants, because of its compatibility with human tissues. Thus, the incorporation of CNTs in these applications presents a major challenge: CNTs can be toxic to human health. Considerable research has shown that this toxicity can be reduced by chemical functionalization or by coating the nanotube surface with substances such as polymer or collagen (Barabás et al. 2015).

Barabás et al. (2015) prepared nanocomposites with –COOH-functionalized CNT/hydroxyapatite and silica substituted hydroxyapatite. The samples were prepared with different methods (coprecipitation, mechanical stirring in ethyl alcohol, and mechanical stirring in Triton X-100) and different MWCNT contents. Their results showed the addition of MWCNT to HAP changed the material properties. The coprecipitation method produced a more homogeneous material in terms of dispersion of the MWCNTs. In vitro bioactivity tests suggested that the addition of MWCNT resulted in a decrease in the hydroxyapatite layer growth during the immersion in simulated body fluid (SBF), which means that higher biocompatibility was achieved.

2.1.4.5 Biomedical Applications

Recently, there has been great interest in using CNTs in biomedicine, which is a field that covers concepts of nanotechnology, biology, and medicine (Oliveira et al. 2015; Beg et al. 2010). Functionalized CNTs are capable of increasing the electrochemical reactivity of important biomolecules, promoting the direct electron

transfer reaction of proteins. Therefore, functionalized CNTs are the focus point for wide range of electrochemical biosensors (Lawal 2016). Biosensors are extremely important for the detection of biological phenomena in medicine (Kruss et al. 2013). Some functionalized CNTs can detect several molecules in biomedicine, such as DNA, adenosine 5-triphosphate (ATP), O_2, N_2, H_2O_2, NO, protein, biomarker, and glucose. (Kruss et al. 2013). In addition, surface-modified CNTs are also studied as nanodrug delivery vectors. They are able to easily cross the cell membranes and exhibit blood circulation half-lives in order of hours. CNT can interact with drugs in three different mechanisms: modification of the surface of drug molecules using covalent or non-covalent bonding, absorption of active drug components on CNT structures, and using CNT channels as catheters (Mehra et al. 2014).

The delivery of proteins, peptides, nucleic acids, and drugs was studied concerning different medical applications (Mehra and Jain 2013; Lu et al. 2012; Qin et al. 2011; Wang et al. 2011; Mehra et al. 2014; Hadidi et al. 2013).

The application of functionalized CNTs has increased in the field of mechanics, electronics, optics, biotechnology, as well as in other areas. With further research, many other innovative applications will be developed. This is a material with unique and exceptional properties, with great potential to surprise us in the future with some new applications.

2.1.5 Characterization of Functionalized Carbon Nanotubes

2.1.5.1 Raman Spectroscopy

Raman spectroscopy is one of the most powerful methods to determine the degree of defect in carbon materials by quantifying the relative intensity of D band ($\sim$1340 cm^{-1}) and graphite G band ($\sim$1570 cm^{-1}). The G band corresponds to the symmetric E2g mode of the graphite hexagonal lattices, while the non-hexagonal structures and the defects caused by a disorder contribute to the D band (Zhang and Xu 2015; Okutan et al. 2014; Hussain et al. 2014). Raman spectrum provides information related to the structural changes of CNT, a direct evidence of its chemical functionalization. Raman also reveals the surface chemistry of the nanotubes (i.e., relative concentration of sp^2- and sp^3-bonded carbon atoms on the surface of the nanotubes) (Kaur et al. 2015). For isolated CNTs, G band reveals only two lines at $\sim$1570 and $\sim$1590 cm^{-1}. The band G width changes and peaks at lower wave numbers are no longer observed (Husanu et al. 2008).

An increase in the D/G intensity ratio (ID/IG) is always considered an indicator of successful covalent functionalization, including oxidation, which can cause an increase in the structural defects of CNT (Zhang and Xu 2015; Kasperski et al. 2014; Kaur et al. 2015). The ratio (ID/IG) increased from 0.16 to 0.40 after an acid covalent functionalization due to sp^2 structure disruption of CNTs by the covalent attachment of functional groups during functionalization. However, a non-covalent

functionalization (with 1-aminopyrene) showed no significant change in ID/IG (from 0.16 to 0.2), maintaining the CNT structure (Jin et al. 2013).

Okutan et al. (2014) showed no changes in the ID/IG of non-covalent functionalized CNT (with dendrimeric cyclophosphazene) after the formation of a nanocomposite material, indicating that non-covalent modification of CNTs does not modify the CNT structure.

Ponnamma et al. (2014) exhibited Raman results of suspensions with pristine and functionalized CNTs that showed mainly 3 peaks. The neat MWCNTs are characterized by three peaks at 1346, 1583, and 2697 cm^{-1}, representing the D, G, and G' bands, respectively. The G band is typical for all graphite-like materials and is assigned to the in-plane vibration of C–C bonds. D band is due to the disorders in carbon systems, and the G' band is the overtone of the D band. After functionalization, all bands are shifted toward higher wave numbers, which indicates the debundling of CNTs. The SDS (sodium dodecyl sulfate) incorporation on CNT surfaces shifts those three bands to 1348, 1585, and 2701 cm^{-1}, together with bandwidth narrowing, showing dispersion improvement.

2.1.5.2 Fourier Transform Infrared Spectroscopy Analysis (FTIR)

FTIR spectra of pure CNT do not exhibit any of the characteristic peaks of organic or inorganic chemical groups (Khan et al. 2010; Fu et al. 2011). In some cases, peaks at around 980 and 3430 cm^{-1} are present due to the presence of OH groups, which are believed to be the result of the adsorption of atmospheric moisture or remains of some purification processes. Peaks in the range of 1550–1700 cm^{-1} may occur as well, which are assigned to the C = C bonds of aromatic rings on the nanotube walls (Zhang et al. 2012b; Behnam et al. 2013).

FTIR spectrum showed bands at about 1040, 1625, 2850, 2920, and 3410 cm^{-1} for CNT functionalized with $H_2NCH_2CH_2O$ group. Bands at about 1040 and 1625 cm^{-1} are related to the C–N stretching vibration and the scissoring in-plane N–H of free primary amine group, respectively. Bands at 2850 and 2920 cm^{-1} are assigned to the symmetrical and asymmetrical stretching of $-CH_2$. Finally, that broad band at $\sim$3410 cm^{-1} is attributed to the NH_2 stretching (Li et al. 2008). Therefore, the presence of the $H_2NCH_2CH_2O$ group together with the CNT sample can be confirmed by FTIR.

The FTIR spectrum of CNT dispersed in sodium dodecyl sulfate (SDS) shows peaks at about 1100, 1400, 2905, and 2980 cm^{-1}. That peak at around 1100 cm^{-1} is assigned to the SO_4 group, while that at 1400 cm^{-1} corresponds to the scissoring and bending of C–H bonds. Those peaks at about 2905 and 2980 cm^{-1} are attributed to the stretching of C–H bonds. The presence of those peaks indicates that SDS successfully coated the CNTs (Khan et al. 2010).

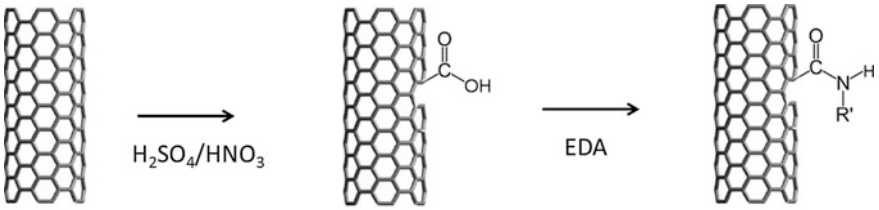

Fig. 2.11 CNT functionalization with acids and EDA (Cividanes et al. 2013)

FTIR spectrum of CNT treated by a mixture of sulfuric acid/nitric acid shows peaks at around 1218, 1580, 1715–1730, 2860, 2930, and 3450 cm^{-1}. That peak at 1218 cm^{-1} was related to the stretching of –C–O groups, while the peak at 1580 cm^{-1} was assigned to –COO asymmetric stretching, the peak at 1715–1730 cm^{-1} was assigned to the stretching of C=O groups, the peak at 2860 and 2930 cm^{-1} was attributed to the asymmetric and symmetric stretching of C–H groups, and the peak at 3450 cm^{-1} was related to the stretching of O–H groups. That peak at 1580 cm^{-1} indicates the introduction of oxygen-containing functional groups during the acid treatment of CNTs (Khan et al. 2010; Xu et al. 2014; Moya et al. 2015; Ahmadzadeh Tofighy and Mohammadi 2015).

For the SO_3H group, absorption bands at ~1005, ~1035, and ~1120 cm^{-1} are present on the FTIR spectra. The broad band at ~3415 cm^{-1} corresponds to the stretch motion absorption of O–H group. Additionally, a C=O stretching at ~1705 cm^{-1} is independent of SO_3H surface incorporation, and it is possibly caused by the oxidation of the terminal CNTs (Fu et al. 2011).

Cividanes et al. (2013) prepared CNTs functionalyzed with ethylenediamine (EDA), undergoing an acid treatment with HNO_3/H_2SO_4 solution. Figure 2.11 shows the squema of the chemical treatment.

After the acid treatment, there is a carboxyl group attached to CNTs, and an amide group is attached after the EDA treatment. The authors determined EDA molecules were covalently bonded to CNT using FTIR spectrum. The sample treated only with acids showed a peak at 1722 cm^{-1}, which is the characteristic of C=O stretching of the carboxylic (COOH) group, and the sample treated with EDA showed a peak at 1670 cm^{-1}, related to C=O stretching of the amide carbonyl, determining that EDA molecules were covalently bonded to acid groups which in turn were covalently bonded to CNT (Cividanes et al. 2013).

2.1.5.3 Thermogravimetric Analysis (TGA)

Thermogravimetric analysis (TGA) can be performed in order to estimate the amount of surface functional groups introduced by oxidizing treatments (Li et al. 2008; Ryu and Han 2014). Oxygen-containing functional groups decompose under higher temperatures, according to the following equations:

$$\mathrm{RCOOH} \rightarrow \mathrm{RH} + \mathrm{CO_2} \tag{2.1}$$

$$\mathrm{RCOH} \rightarrow \mathrm{RH} + \mathrm{CO} \tag{2.2}$$

$$\mathrm{RCOOR} \rightarrow \mathrm{RR} + \mathrm{CO_2} \tag{2.3}$$

The mass loss in the region from room temperature up to 150 °C is related to the release of physisorbed water. Carboxylic acids, amide groups, and dehydration of phenolic groups can be observed in the range from 150 to 300 °C (Kumar and Gasem 2015), followed by decomposition of aldehydes, anhydrides, phenoxy-substituted dendrimeric cyclic phosphazenes and esters up to 600 °C (Okutan et al. 2014), and finally ethers and quinones. Further mass loss can be attributed to the decomposition of carbonyl groups, which can be observed at temperatures higher than 700 °C. However, the determination of decomposition products is more difficult at higher temperatures (Steimecke et al. 2015).

2.1.5.4 X-Ray Photoelectron Spectroscopy (XPS)

X-ray photoelectron spectroscopy (XPS) can be used for studying the evolution of surface chemistry during the oxidation processes. A typical high-resolution C 1 s spectrum shows peaks at ~284.6 eV, which correspond to sp^2-C in C=C bonds, and peaks at ~285.3 eV, related to sp^3-C at the defective sites. Peaks centered at ~286.3, ~287.7, and ~288.9 eV are assigned to oxygenated carbon atoms in C–O, C=O, and O–C=O bonds, respectively. The small peaks above ~291.0 eV are from $\pi \rightarrow \pi^*$ transition (Zhang and Xu 2015).

A usual high-resolution O 1 s spectrum shows peaks at ~531.5–533.8 eV and was used to analyze the surface oxygen functional groups. Peaks at ~532.8–533.8 eV are related to carbon-oxygen single bonds (C–O), which are due to the presence of alcohols and/or ethers on the CNT surface. Peaks at ~531.5–532.5 eV dominated the O 1 s region, and they are the characteristics of doubly bound oxygen (C=O), which is present in aldehydes, ketones, carboxylic acids, and their derivatives (Steimecke et al. 2015).

2.1.5.5 X-Ray Diffraction (XRD)

CNTs mostly consist of crystalline and amorphous phases. All units for XRD peak position are at 2θ unit. The characteristic peaks in X-ray diffraction are at: ~26° (graphitic plane 002), ~42.5° (graphitic plane 100), ~53.5° (graphitic plane 004), and ~77° (graphitic plane 110). In certain cases, some peaks related to metallic catalyst are also present. Peaks of some iron phases (Fe_3C, α-Fe, and γ-Fe–C) are at 38°–50°, and they are likely to be present when iron is used as catalyst (Antunes et al. 2011) (Safari and Zarnegar 2013).

A series of chemical modifications can decrease the crystalline degree of CNTs due to the creation of some defects on the CNT walls. A peak broadening and/or a decrease in peak intensity indicates either a presence of a strain on the CNT surface or a reduction in the CNT diameter (Yang et al. 2009; Nair et al. 2015).

2.1.5.6 Dispersion of Functionalized CNTs in Different Solvents

Small quantities of CNTs are added into flasks and then sonicated in a low-power and high-frequency sonicator bath to determine the functionalization capability of dispersing CNTs (Fig. 2.12) in a chosen solvent.

Good dispersion and time stability are evaluated in this test. Thus, this is a simple test for evaluating the CNT dispersion in relation to the presence of a functionalization group.

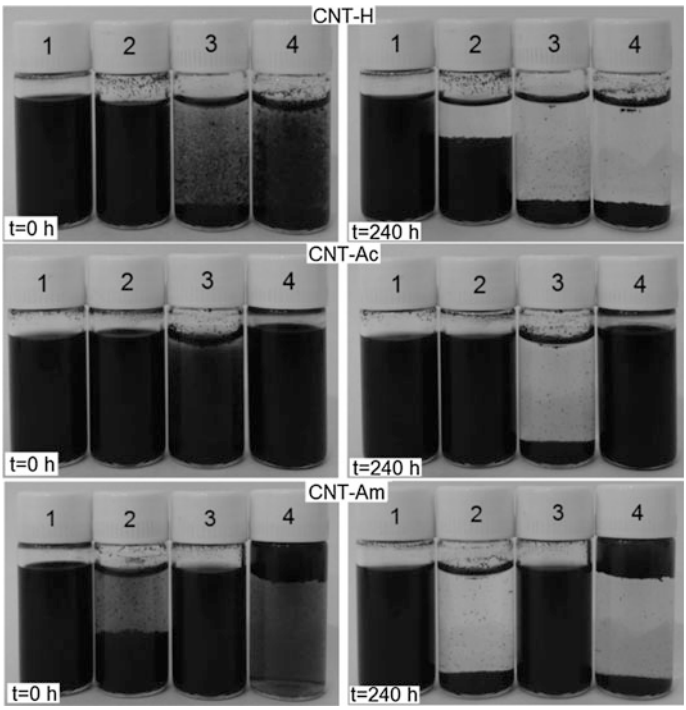

Fig. 2.12 Images of CNT treated with **a** HCl, **b** H_2SO_4 + HNO_3, **c** Dodecylamine (DDA), in the solvents: *1* acetone, *2* ethanol, *3* xylene, *4* water, after sonication for 1 h (Ferreira et al. 2015)

References

Abdalla M, Dean D, Robinson P et al (2008) Cure behavior of epoxy/MWCNTs nanocomposites: the effect of nanotube surface modification. Polymer 49:3310–3317

Ahmadzadeh Tofighy M, Mohammadi T (2015) Nickel ions removal from water by two different morphologies of induced CNTs in mullite pore channels as adsorptive membrane. Ceram Int 41 (4):5464–5472

Ajayan PM, Stephan O, Colliex C et al (1994) Aligned carbon nanotube arrays formed by cutting a polymer resin-nanotube composite. Science 265:1212–1214

Alpatova AL, Shan W, Babica P et al (2010) Single-walled carbon nanotubes dispersed in aqueous media via non-covalent functionalization: effect of dispersant on the stability, cytotoxicity, and epigenetic toxicity of nanotube suspensions. Water Res 44(2):505–520

Ando Y, Zhaob X, Hiraharab K et al (2000) Mass production of single-wall carbon nanotubes by the arc plasma jet method. Chem Phy Lett 323:580–585

Ansari R, Ajori S, Rouhi S (2015) Elastic properties and buckling behavior of single-walled carbon nanotubes functionalized with diethyltoluenediamines using molecular dynamics simulations. Superlattices Microstruct 77:54–63

Antunes EF, Resende VG, Mengui UA et al (2011) Analyses of residual iron in carbon nanotubes produced by camphor/ferrocene pyrolysis and purified by high temperature annealing. Appl Surf Sci 257(18):8038–8043

Arora N, Sharma NN (2014) Arc discharge synthesis of carbon nanotubes: comprehensive review. Diam Rel Mat 50:135–150

Badhulika S, Myung NV, Mulchandani A (2014) Conducting polymer coated single-walled carbon nanotube gas sensors for the detection of volatile organic compounds. Talanta 123:109–114

Bai JB, Hamon A-L, Marraud A, Jouffrey B, Zymla V (2002) Synthesis of SWCNTs and MWCNTs by a molten salt (NaCl) method. Chem Phys Lett 365:184–188

Balasubramanian K, Burghard M (2005) Chemically functionalized carbon nanotubes. Small 1:180–192

Barabás R, Katona G, Bogya ES et al (2015) Preparation and characterization of carboxyl functionalized multiwall carbon nanotubes–hydroxyapatite composites. Ceram Int 41:12717–12727

Baskaran D, Mays JW, Bratcher MS (2004) Polymer-grafted multiwalled carbon nanotubes through surface-initiated polymerization. Angew Chem Int Ed 43:2138–2142

Beg S, Rizwan M, Sheikh AM (2010) Advancement in carbon nanotubes: basics, biomedical applications and toxicity. J Pharmacy Pharmac 63:141–163

Behnam B, Shier WT, Nia AH et al (2013) Non-covalent functionalization of single-walled carbon nanotubes with modified polyethyleneimines for efficient gene delivery. Int J Pharm 454 (1):204–215

Bolshakov AP, Uglov SA, Saveliev AV et al (2002) A novel CW laser–powder method of carbon single-wall nanotubes production. Diam Rel Mat 11:927–930

Boujtita M (2014) Nanosensors for chemical and biological applications. 1—chemical and biological sensing with carbon nanotubes (CNTs). Woodhead Publishing Limited, Sawston, pp 3–27

Bounioux C, Katz EA, Yerushalmi-Rozen R (2012) Conjugated polymers—carbon nanotubes-based functional materials for organic photovoltaics: a critical review. Polym Adv Technol 23:1129–1140

Byrappa K, Adschiri T (2007) Hydrothermal technology for nanotechnology. Prog Cryst Growth Charact Mater 53:117–166

Cakmak G, Guney HY, Yuksel SA et al (2015) The effect of functionalized single walled carbon nanotube with octadecylamine on efficiency of poly-(3-hexylthiophene): [(6,6)] phenyl C61 butyric acid methyl ester organic solar cells. Phys B: Condens Matter 461:85–91

Cesano F, Rattalino I, Demarchi D et al (2013) Structure and properties of metal-free conductive tracks on polyethylene/multiwalled carbon nanotube composites as obtained by laser stimulated percolation. Carbon 61:63–71
Chen GX, Kim HS, Park BH et al (2007) Synthesis of poly(L-lactide)-functionalized multiwalled carbon nanotubes by ring-opening polymerization. Macromol Chem Phys 208:389–398
Chen X, Yu X, Liu Y et al (2013) Stepwise design of non-covalent wrapping of large diameter carbon nanotubes by peptides. J Mol Graph Model 46:83–92
Cividanes LS, Brunelli DD, Antunes EF et al (2013) Cure study of epoxy resin reinforced with multiwalled carbon nanotubes by Raman and luminescence spectroscopy. J Appl Polym Sci 127:544–553
Cividanes LS, Simonetti EAN, Moraes MB et al (2014a) Influence of carbon nanotubes on epoxy resin cure reaction using different techniques: a comprehensive review. Pol Eng Sci 54:2461–2469
Cividanes LS, Simonetti EAN, De Oliveira JIS et al (2015) The sonication effect on CNT-epoxy composites finally clarified. Polym Compos. doi:10.1002/pc.23767
Cividanes LS, Simonetti EA, Campos TM et al (2014b) Anomalous behavior of thermal stability of amino-carbon nanotube-epoxy nanocomposite. J Comp Mat 49:3067–3073
Coleman J, Khan U, Gun'ko Y (2006) Mechanical reinforcement of polymers using carbon nanotubes. Adv Mater 18(6):689–706
De Filpo G et al (2015) Non-covalent functionalisation of single wall carbon nanotubes for efficient dye-sensitised solar cells. J Power Sources 274:274–279
De Greef N, Zhang L, Magrez A et al (2015) Direct growth of carbon nanotubes on carbon fibers: effect of the CVD parameters on the degradation of mechanical properties of carbon fibers. Diam Relat Mater 51:39–48
De Volder MFL, Tawfick SH, Baughman RH et al (2013) Carbon nanotubes: present and future commercial applications. Science 339:535–539
Ferreira FV, Francisco W, Menezes BRC et al (2015) Carbon nanotube functionalized with dodecylamine for the effective dispersion in solvents. Appl Surf Sci 357:2154–2159
Francisco W, Ferreira FV, Ferreira EV et al (2015) Functionalization of multi-walled carbon nanotube and mechanical property of epoxy-based nanocomposite. J Aerosp Technol Manag 7:289–293
Fu Q, Gao B, Dou H et al (2011) Novel non-covalent sulfonated multiwalled carbon nanotubes from p-toluenesulfonic acid/glucose doped polypyrrole for electrochemical capacitors. Synth Met 161(5–6):373–378
Ghosh A, Rao KV, Voggu R et al (2010) Non-covalent functionalization, solubilization of graphene and single-walled carbon nanotubes with aromatic donor and acceptor molecules. Chem Phys Lett 488(4–6):198–201
Goddard WA, Brenner D, Lyshevski SE et al (2012) Handbook of nanoscience, engineering, and technology, 3rd edn. Taylor & Francis Group, London, 1093p
Gogotsi Y, Libera JA, Yoshimura M (2000) Hydrothermal synthesis of multiwall carbon nanotubes. J Mater Res 15:2591–2594
Gogotsi Y, Naguib N, Libera J (2002) In situ chemical experiments in carbon nanotubes. Chem Phys Lett 365:354–360
Gogotsi Y, Presser V (2013) Carbon nanomaterials. 2nd edn. Taylor & Francis Group, London, 529p
Gohardani O, Elola MC, Elizetxea C (2014) Potential and prospective implementation of carbon nanotubes on next generation aircraft and space vehicles: a review of current and expected applications in aerospace sciences. Prog Aerosp Sci 70:42–68
González-Gaitán C, Ruiz-Rosas R, Morallón E et al (2015) Functionalization of carbon nanotubes using aminobenzene acids and electrochemical methods. Electroactivity for the oxygen reduction reaction. Int J Hydrogen Energy 40:11242–11253
González-Gaitán C, Ruiz-Rosas R, Nishiharab H et al (2016) Successful functionalization of superporous zeolite templated carbon using aminobenzene acids and electrochemical methods. Carbon 99:157–166

Gooding J (2005) Nanostructuring electrodes with carbon nanotubes: a review on electrochemistry and applications for sensing. Electrochim Acta 50:3049–3060

Guo T, Nikolaev P, Thess A et al (1995) Catalytic growth of single-walled nanotubes by laser vaporization. Chem Phys Lett 243:49–54

Hadidi N, Kobarfard F, Nafissi-Varcheh N et al (2013) PEGylated single-walled carbon nanotubes as nanocarriers for cyclosporin A delivery. AAPS Pharm Sci Technol 14:593–600

Hong S, Kim D, Lee S et al (2015) Enhanced thermal and mechanical properties of carbon nanotube composites through the use of functionalized CNT-reactive polymer linkages and three-roll milling. Comp Part A: Appl Sci Manuf 77:142–146

Hsu WK, Terrones M, Hare JP et al (1996) Electrolytic formation of carbon nanostructures. Chem Phys Lett 262:161–166

Huang C, Liao Q, Li Y (2007) Non-covalent anionic porphyrin functionalized multi-walled carbon nanotubes as an optical probe for specific DNA detection. Talanta 75(1):163–166

Husanu M, Baibarac M, Baltog I (2008) Non-covalent functionalization of carbon nanotubes: Experimental evidence for isolated and bundled tubes. Phys E 41(1):66–69

Hussain S, Amade R, Moreno H et al (2014) RF-PECVD growth and nitrogen plasma functionalization of CNTs on copper foil for electrochemical applications. Diamond Relat Mater 49:55–61

Iijima S (1991) Helical microtubules of graphitic carbon. Nature 354:56–58

Iijima S (1993) Growth of carbon nanotubes. Mater Sci Eng B 19:172–180

Jin SH, Cha SL, Jun GH et al (2013) Non-covalently functionalized single walled carbon nanotube/poly(3,4ethylenedioxythiophene):poly(styrenesulfonate) nanocomposites for organic photovoltaic cell. Synthetic Met 181:92–97

Jorio A, Dresselhaus G, Dresselhaus MS (2008) Carbon nanotubes advanced topics in the synthesis, structure, properties and applications. Springer, Heidelberg, p 709p

Kabbani MA, Tiwary CS, Autreto PAS et al (2015) Ambient solid-state mechano-chemical reactions between functionalized carbon nanotubes. Nat Commun 6:7291

Kasperski A, Weibel A, Estournès C et al (2014) Multi-walled carbon nanotube–Al_2O_3 composites: covalent or non-covalent functionalization for mechanical reinforcement. Scr Mater 75:46–49

Kaur A, Singh I, Kumar J et al (2015) Enhancement in the performance of multi-walled carbon nanotube: poly(methylmethacrylate) composite thin film ethanol sensors through appropriate nanotube functionalization. Mater Sci Semicond Process 31:166–174

Khan MU, Gomes VG, Altarawneh IS (2010) Synthesizing polystyrene/carbon nanotube composites by emulsion polymerization with non-covalent and covalent functionalization. Carbon 48(10):2925–2933

Kroto HW, Heath JR, O'Brien SC et al (1985) C_{60}: bulkerminsterfullerene. Nature 318:162–163

Kruss S, Hilmer AJ, Zhang J et al (2013) Carbon nanotubes as optical biomedical sensors. Adv Drug Deliv Rev 65:1933–1950

Kuang Y, Huang B (2015) Effects of covalent functionalization on the thermal transport in carbon nanotube/polymer composites: a multi-scale investigation. Polymer 56:563–571

Kumar B, Castro M, Feller JF (2012) Poly(lactic acid)-multi-wall carbon nanotube conductive biopolymer nanocomposite vapour sensors. Sens Act B Chem 161:621–628

Kumar M, Ando Y (2010) Chemical vapor deposition of carbon nanotubes: a review on growth mechanism and mass production. J Nanosci Nanotech 10:3739–3758

Lawal AT (2016) Synthesis and utilization of carbon nanotubes for fabrication of electrochemical biosensors. Mater Res Bull 73:308–350

Lee JU, Huh J, Kim KH et al (2007) Aqueous suspension of carbon nanotubes via non-covalent functionalization with oligothiophene-terminated poly(ethylene glycol). Carbon 45(5):1051–1057

Lee SW (2015) Mechanical properties of suspended individual carbon nanotube studied by atomic force microscope. Synthetic Met. Available online 28 Sept 2015 (in press)

Li Q, Yan H, Zhang J et al (2004) Effect of hydrocarbons precursors on the formation of carbon nanotubes in chemical vapor deposition. Carbon 42:829–835

Li WZ, Xie SS, Qian LX et al (1996) Large scale synthesis of aligned carbon nanotubes. Science 274:1701–1703

Li X et al (2008) Non-covalent functionalization of multi walled carbon nanotubes and their application for conductive composites. Carbon 46:818–832

Liu W-W, Chai S-P, Mohamedc AR et al (2014) Synthesis and characterization of graphene and carbon nanotubes: a review on the past and recent developments. J Ind Eng Chem 20:1171–1185

Liu Y, Chi W, Duan H et al (2016) Property improvement of room temperature vulcanized silicone elastomer by surface-modified multi-walled carbon nanotube inclusion. J Alloys Compd 657:472–477

Loos M, Schulte K (2015) Is it worth the effort to reinforce polymers with carbon nanotubes? Carbon nanotube reinforced composites (Chap. 8), 1st edn. Elsevier, Waltham, p 304p

Lu Y, Ye G, Wang Y (2012) The Darboux problem involving the distributional Henstock-Kurzweil integral. Proc Edinburgh Math Soc 55:197–205

Ma PC, Siddiqui NA, Marom G et al (2010) Dispersion and functionalization of carbon nanotubes for polymer-based nanocomposites: a review. Compos Part B: Appl Sci Manuf 41:1345–1367

Madec L, Humbert B, Lestriez B et al (2013) Covalent vs. non-covalent redox functionalization of C-LiFePO4 based electrodes. J Power Sources 232:246–253

Kumar AM, Gasem ZM (2015) Effect of functionalization of carbon nanotubes on mechanical and electrochemical behavior of polyaniline nanocomposite coatings. Surf Coat Technol 276:416–423

Mehra NK, Jain NK (2013) Development, characterization and cancer targeting potential of surface engineered carbon nanotubes. J Drug Target 21:745–758

Mehra NK, Mishra V, Jain NK (2014) A review of ligand tethered surface engineered carbon nanotubes. Biomaterials 35:1267–1283

Meng L, Fu C, Lu Q (2009) Advanced technology for functionalization of carbon nanotubes. Prog Nat Sci 19:801–810

Mittal G, Dhand V, Rhee KY (2015) A review on carbon nanotubes and graphene as fillers in reinforced polymer nanocomposites. J Ind Eng Chem 21:11–25

Mittal V (2011) Carbon nanotubes surface modifications: an overview. Wiley-VCH Verlag GmbH & Co., Weinheim, 24p

Mohamed A, Anas AK, Bakar SA et al (2015) Enhanced dispersion of multiwall carbon nanotubes in natural rubber latex nanocomposites by surfactants bearing phenyl groups. J Colloid Interf Sci 455:179–187

Moniruzzaman M, Winey KI (2006) Polymer nanocomposites containing carbon nanotubes. Macromolecules 39:5194–5205

Montazareli A, Naghdabadi R (2009) Study the effect of viscoelastic matrix model on the stability of CNT/Polymer composites by multiscale modeling. Polym Compos 30:1545–1551

Moreno JMC, Swamy SS, Fujino T et al (2000) Carbon nanocells and nanotubes grown in hydrothermal fluids. Chem Phys Lett 329:317–322

Moya A, Cherevan A, Marchesan S et al (2015) Oxygen vacancies and interfaces enhancing photocatalytic hydrogen production in mesoporous CNT/TiO_2 hybrids. Appl Catal B 179:574–582

Nair LG, Mahapatra AS, Gomathi N et al (2015) Radio frequency plasma mediated dry functionalization of multiwall carbon nanotube. Appl Surf Sci 340:64–71

Okutan E, Çosut B, Kayiran SB et al (2014) Synthesis of a dendrimeric phenoxy-substituted cyclotetraphosphazene and its non-covalent interactions with multiwalled carbon nanotubes. Polyhedron 67:344–350

Oliveira SF, Bisker G, Bakh N et al (2015) Protein functionalized carbon nanomaterials for biomedical applications. Carbon 95:767–779

Paradise M, Goswami T (2007) Carbon nanotubes—production and industrial applications. Mater Design 28:1477–1489

Park SJ, Cho MS, Lim ST et al (2003) Synthesis and dispersion characteristics of multi-walled carbon nanotube composites with poly(methyl methacrylate) prepared by in-situ bulk polymerization. Macromol Rapid Commun 24:1070–1073

Perry A, Green SJ, Horsell DH et al (2015) A pyrene-appended spiropyran for selective photo-switchable binding of Zn(II): UV–visible and fluorescence spectroscopy studies of binding and non-covalent attachment to graphene, graphene oxide and carbon nanotubes. Tetrahedron 71(38):6776–6783

Pillet J-D, Quay CHL, Morfin P et al (2010) Andreev bound states in supercurrent-carrying carbon nanotubes revealed. Nat Phys 6:965–969

Polo-Luque ML, Simonet BM, Valcárcel M (2013) Functionalization and dispersion of carbon nanotubes in ionic liquids. TrAC, Trends Anal Chem 47:99–110

Ponnamma D, Sung SH, Hong JS et al (2014) Influence of non-covalent functionalization of carbon nanotubes on the rheological behavior of natural rubber latex nanocomposites. Eur Polym J 53:147–159

Prasek J, Drbohlavova J, Chomoucka J et al (2011) Methods for carbon nanotubes synthesis—review. J Mater Chem 21:15872–15884

Qin W, Yang K, Tang H et al (2011) Improved GFP gene transfection mediated by polyamidoamine dendrimer-functionalized multi-walled carbon nanotubes with high biocompatibility. Colloid Surf B 84:206–213

Rahmat M, Hubert P (2011) Carbon nanotube–polymer interactions in nanocomposites: a review. Comp Sci Technol 72:72–84

Ren Z, Lan Y, Wang Y (2012) Aligned carbon nanotubes: physics, concepts, fabrication and devices. Springer Science & Business Media, Berlin 300p

Ryu J, Han M (2014) Improvement of the mechanical and electrical properties of polyamide 6 nanocomposites by non-covalent functionalization of multi-walled carbon nanotubes. Comp Sci Technol 102:169–175

Sa N, Wang G, Yin B et al (2008) Theoretical study on non-covalent functionalization of armchair carbon nanotube by tetrathiafulvalene molecule. Phys E 40(7):2396–2399

Safari J, Zarnegar Z (2013) Synthesis of amidoalkyl naphthols by nano-Fe_3O_4 modified carbon nanotubes via a multicomponent strategy in the presence of microwaves. J Ind Eng Chem 20:2292–2297

Sahoo NG, Rana S, Cho JW et al (2010) Polymer nanocomposites based on functionalized carbon nanotubes. Prog Polymer Sci 35:837–867

Sanz V, Borowiak E, Lukanov P et al (2011) Optimising DNA binding to carbon nanotubes by non-covalent methods. Carbon 49(5):1775–1781

Shaffer MSP, Windle AH (1999) Fabrication and characterization of carbon nanotube/poly (vinyl alcohol) composites. Adv Mater 11:937–941

Shah KA, Tali BA (2016) Synthesis of carbon nanotubes by catalytic chemical vapour deposition: a review on carbon sources, catalysts and substrates. Mater Sci Semicond Process 41:67–82

Shi X, Jiang B, Wang J et al (2012) Influence of wall number and surface functionalization of carbon nanotubes on their antioxidant behavior in high density polyethylene. Carbon 50:1005–1013

Shimotani K, Anazawa K, Watanabe H et al (2001) New synthesis of multi-walled carbon nanotubes using an arc discharge technique under organic molecular atmospheres. Appl Phys A 73:451–454

Song JL, Wang L, Feng SA et al (2009) Growth of carbon nanotubes by the catalytic decomposition of methane over Fe-Mo/Al_2O_3 catalyst: effect of temperature on tube structure. New Carbon Mater 24:307–313

Steimecke M, Rümmler S, Bron M (2015) The effect of rapid functionalization on the structural and electrochemical properties of high-purity carbon nanotubes. Electrochim Acta 163:1–8

Szabó A, Perri C, Csató A et al (2010) Synthesis methods of carbon nanotubes and related materials. Materials 3:3092–3140

Terrones M (2003) Science and technology of the twenty-first century: synthesis, properties, and applications of carbon nanotubes. Annu Rev Mater Res 33:419–501

Thess A, Lee R, Nikolaev P et al (1996) Crystalline ropes of metallic carbon nanotubes. Science 273:483–487

Thostenson ET, Ren Z, Chou TW (2001) Advances in the science and technology of carbon nanotubes and their composites: a review. Compos Sci Technol 61:1899–1912

Tsierkezos NG, Ritter U, Thaha YN et al (2015) Application of multi-walled carbon nanotubes modified with boron oxide nanoparticles in electrochemistry. Ionics 21:3087–3095

Verma SK, Kar P, Yang DJ et al (2015) Poly(m-aminophenol)/functionalized multi-walled carbon nanotube nanocomposite based alcohol sensors. Sens Actuartor B 219:199–208

Wang L, Zhang M, Chang N et al (2011) Synergistic enhancement of cancer therapy using a combination of docetaxel and photothermal ablation induced by single-walled carbon nanotubes. Int J Nanomed 6:2641–2652

Wang Q, Arash B (2014) A review on applications of carbon nanotubes and graphenes as nano-resonator sensors. Comput Mater Sci 82:350–360

Wang S, Liang R, Wang B et al (2008) Reinforcing polymer composites with epoxide-grafted carbon nanotubes. Nanotechnology 19:085710 (7 pp)

Wang Z, Colorado HA, Guo Z-H et al (2012) Effective functionalization of carbon nanotubes for bisphenol F epoxy matrix composites. Mater Res 15:510–516

Wong BS, Yoong SL, Jagusiak A et al (2013) Carbon nanotubes for delivery of small molecule drugs. Adv Drug Deliv Rev 65:1964–2015

Xia H, Zhang Y, Chen C et al (2016) Ozone-mediated functionalization of multi-walled carbon nanotubes and their activities for oxygen reduction reaction. J Mater Sci Technol. Available online 6 Jan 2016 (in press)

Xu D, Li B, Wei C et al (2014) Preparation and characterization of MnO_2/acid-treated CNT nanocomposites for energy storage with zinc ions. Electrochim Acta 133:254–261

Yang W, Ratinac KR, Ringer SP et al (2010) Carbon nanomaterials in biosensors: should you use nanotubes or graphene biosens. Carbon Nanomater 49:2114–2138

Yang K, Gu M, Guo Y et al (2009) Effects of carbon nanotube functionalization on the mechanical and thermal properties of epoxy composites. Carbon 47(7):1723–1737

Zaman AC, Ustundag CB, Kaya F et al (2012) OH and COOH functionalized single walled carbon nanotubes-reinforced alumina ceramic nanocomposites. Cerm Int 38:1287–1293

Zeng HL, Gao C, Yan DY (2006) Poly(L-caprolactone)-functionalized carbon nanotubes and their biodegradation properties. Adv Funct Mater 16:812–818

Zhang A, Luan J, Zheng Y et al (2012a) Effect of percolation on the electrical conductivity of amino molecules non-covalently coated multi-walled carbon nanotubes/epoxy composites. Appl Surf Sci 258(22):8492–8497

Zhang A, Tang M, Luan J et al (2012b) Noncovalent functionalization of multi-walled carbon nanotubes with amphiphilic polymers containing pyrene pendants. Mater Lett 67(1):283–285

Zhang F, Ren P, Pan X et al (2015) Self-assembly of atomically thin and unusual face-centered cubic Re nanowires within carbon nanotubes. Chem Mater 27:1569–1573

Zhang Z, Xu X (2015) Nondestructive covalent functionalization of carbon nanotubes by selective oxidation of the original defects with K_2FeO_4. Appl Surf Sci 346:520–527

Zhao Z, Zhou Y, Zhang C et al (2015) Thermoset composites functionalized with carbon nanofiber sheets for EMI shielding. Appl Polym Sci 132:41873

Conclusions

This book describes the main types of functionalization of graphene and carbon nanotubes, inlcuding the functionalization types as follows: covalent, non-covalent and others. The book also summarizes the key techniques of characterization of functionalized materials, in addition to the main applications of each one. With a critical view and recent literature, the goal was to bring the reader the most relevant information on the subject.

F.V. Ferreira et al., *Functionalizing Graphene and Carbon Nanotubes*,
SpringerBriefs in Applied Sciences and Technology,
DOI 10.1007/978-3-319-35110-0